

SHEAR FATIGUE BEHAVIOR OF STEEL-CONCRETE SANDWICH BEAMS

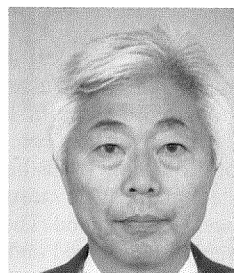
(Translation from Proceedings of JSCE, No.585/V-38, February 1998)



Tamon UEDA



Mohab ZAHRAN



Yoshio KAKUTA

Fatigue tests were carried out on steel-concrete sandwich beams with and without shear reinforcement. Under fatigue loading, the sandwich beams exhibited various failure modes with either concrete fatigue failure or steel fatigue fracture. The *S-N* relationship for the different failure modes is presented. The fatigue strength of the sandwich beams was also predicted by a finite element method in which constitutive laws were modified based on the experimental results of concrete in fatigue loading. Based on the results of this study, a fatigue design proposal for sandwich beams both with and without shear reinforcement is also presented.

Keywords : *fatigue strength, finite element analysis, shear reinforcement, steel-concrete sandwich beam*

Tamon UEDA is an associate professor at the Division of Structural & Geotechnical Engineering of Hokkaido University, Sapporo, Japan. He obtained his D. Eng. from the University of Tokyo in 1982. His research interest is the structural analysis of composite and retrofitted concrete structures. He is a member of the JSCE.

Mohab ZAHRAN is a design engineer at DAR AL-HANDASAH Consultants, Egypt. He obtained his D. Eng. from Hokkaido University in 1996 and worked with Sumitomo Construction for two years.

Yoshio KAKUTA is a professor at the Division of Structural & Geotechnical Engineering of Hokkaido University, Sapporo, Japan. He obtained his D. Eng. from Hokkaido University in 1968. His research interest is the design and analysis of hybrid structures. He is a fellow of the JSCE.

1. INTRODUCTION

Recently, the application of composite structures has become increasingly common. A new type of composite structure, the steel-concrete sandwich structure, has been developed to fulfill complicated structural requirements. As shown in Fig.1, a steel-concrete sandwich member comprises a core of concrete, flange steel plates, shear reinforcing steel plates, and shear connectors (i.e., steel angles) to transfer the shear from the concrete to the flange plates. Such sandwich members offer higher load-carrying capacity and higher ductility than comparable ordinary RC members. The sandwich member has also proved good as regards constructability since the cost of formwork and the period of construction can be considerably reduced.

Sandwich members have practical application in various structures such as tunnels, bridge decks, marine structures, etc. Marine structures are subjected to continuous cyclic wave forces. Bridge decks are also subjected to repeated traffic loading. These repetitive loads may result in progressive cracking and sometimes crushing of the core concrete if the load amplitude is sufficiently large. Further, a sandwich member has many welds between steel plates and steel angles, and these may lead to fatigue fracture of the steel plates. This means that the fatigue endurance of steel-concrete sandwich members has to be adequately investigated. The flexural capacity and the shear capacity of this type of members has been thoroughly investigated under static loading conditions, leading to the recent proposal of the design code for steel-concrete sandwich structures [1]. However, there has been little research into the fatigue strength of steel-concrete sandwich members [2][3]. This paper presents experimental and analytical studies of the fatigue strength of steel-concrete sandwich beams both with and without shear reinforcement. The study is limited to one-sided cyclic loading.

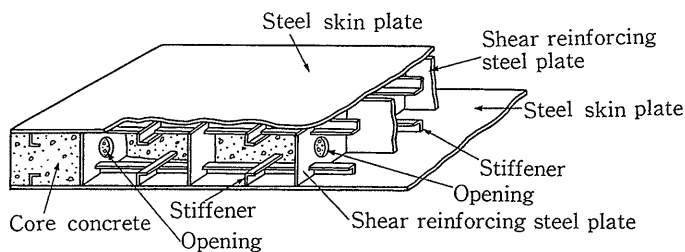


Fig.1 Steel-Concrete Sandwich Member

2. EXPERIMENTAL WORK

2.1 Sandwich Beams Without Shear Reinforcement [4]

Figure 2 shows the steel-concrete sandwich beam without shear reinforcement as investigated in this study. The cross section of this beam is 250×400 mm and its span is 2.65 m. Two symmetrical concentrated loads were applied, and the shear span to effective depth ratio (a/d) was equal to 3.0. The

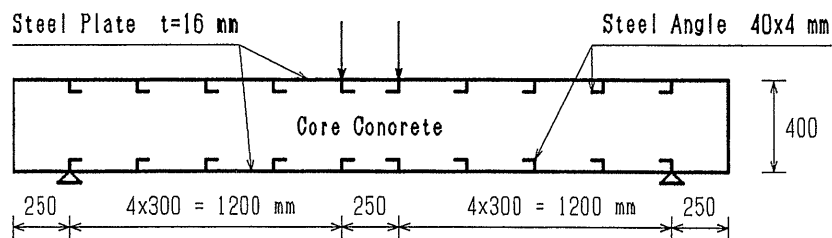


Fig.2 Geometry and Loading Configuration of Sandwich Beam without Shear Reinforcement

thickness of the steel skin plates was 16 mm. The yield strength of the steel plates (f_y) was 400 MPa. The compressive strength of the concrete (f_c') was 25 MPa. Steel angle measuring $40 \times 40 \times 4$ mm was used for shear connectors, and these were welded to the steel skin plates. Tests were carried out on eight specimens. Specimen 1 was tested under static monotonic loading, while the other seven were tested under fatigue loading. In the fatigue tests, the specimens were loaded with a sinusoidal waveform and the loading frequency was 4.0 Hz. The minimum fatigue load (P_{min}) was kept constant at 20 kN, which is about 6% of the static load-carrying capacity of the beam ($P_{u,exp}$). For specimens 2, 3, 4, 5, 6, 7, and 8, the maximum fatigue load (P_{max}) was 38.7%, 49.0%, 63.2%, 70.7%, 82.1%, 43.1%, and 58.5% of $P_{u,exp}$, respectively. For specimen 2, fatigue failure had not occurred by 2×10^6 cycles and therefore the maximum load was increased to 65.5% of $P_{u,exp}$.

2.2 Sandwich Beams With Shear Reinforcement

Experiments were also carried out on the steel-concrete sandwich beam with shear reinforcement shown in Fig.3, which has a span of 1.69 m and a cross section of 150×300 mm. The specimens were tested by applying two symmetrical concentrated loads, and the shear span to effective depth ratio (a/d) was equal to 2.4. The thickness of the upper and lower flange plates was 16 mm. As shown in Fig.3, the sandwich beams were provided with shear reinforcing steel plates. For sandwich beams of type A, the right and left shear spans were reinforced with a vertical steel plate 100 mm in width and 6 mm in thickness. This vertical plate was placed at the center of the shear span parallel to the member axis. For sandwich beams of type B, the right and left shear spans were reinforced with three vertical steel plates each 33 mm in width and 6 mm in thickness. In the right shear span, the vertical plates were placed parallel to the member axis at a spacing of 180 mm. However, in the left shear span, they were placed normal to the

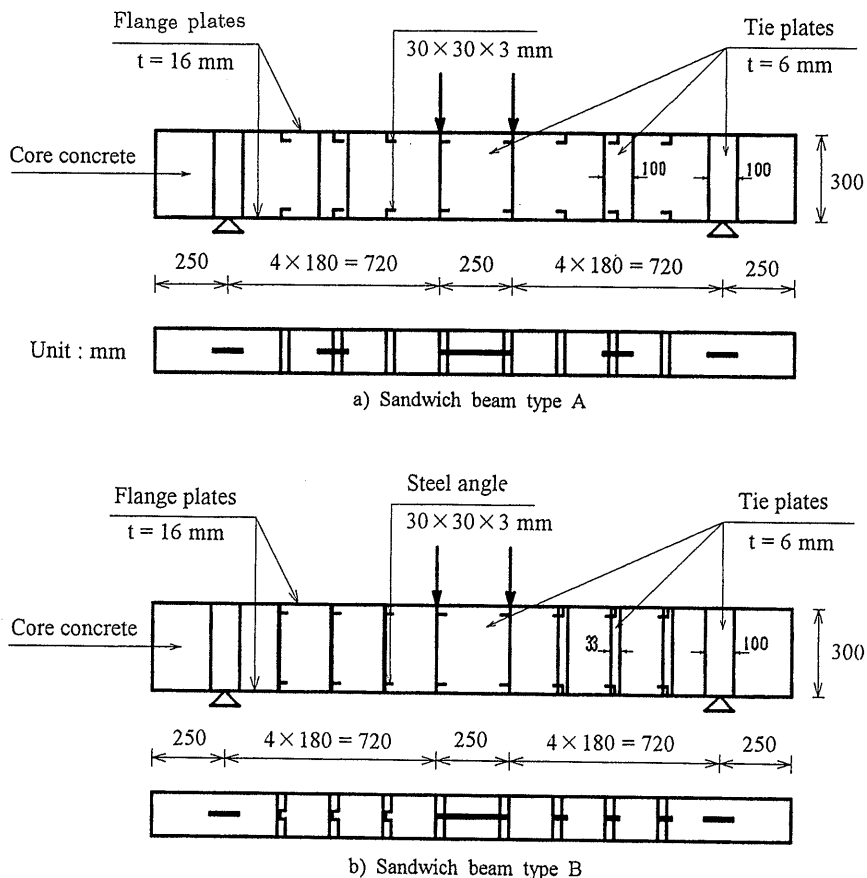


Fig.3 Geometry and Loading Configuration of Sandwich Beams with Shear Reinforcement

member axis at a spacing of 180 mm. These vertical steel plates were welded at their ends to the upper and lower flange plates. These vertical steel plates are known as 'tie plates'. Note that the ratio of shear reinforcement is identical in all shear spans in the sandwich beams under investigation. The flange plates as well as the tie plates were of SM490A steel, which has a yielding point of 400 MPa and a tensile strength of 550 MPa. The average compressive strength of the concrete was 15.4 MPa. The maximum size of aggregate used in the concrete mix was 25 mm. Steel angle measuring 30×30×3 mm was used for shear connectors, which were welded to the flange plates. A V-shaped groove was prepared for welding with full penetration. The welding rod used was designed for high strength steel with a tensile strength greater than 490 MPa.

Tests were carried out on six sandwich beams of type A, identified as A1, A2, A3, A4, A5, and A6. Tests were carried out also on two sandwich beams of type B, which are identified as B1 and B2. First, specimen A1 was tested under static monotonic loading in order to clarify know the static load-carrying capacity of sandwich beams of type A. Sandwich beams of type A and type B were assumed to have the same static load-carrying capacity, since their shear reinforcement ratios were identical.

Next, specimens A2, A3, A4, A5, A6, B1, and B2 were tested under fatigue loading. The minimum fatigue load (P_{min}) was kept constant at 20 kN, which is about 5.5% of the static load-carrying capacity of the beam ($P_{u,exp}$). For specimens A2, A3, A4, A5, A6, B1, and B2, the maximum fatigue load (P_{max}) was equal to 52.5%, 68.3%, 81.1%, 90.4%, 96.1%, 54.3%, and 41.8%, respectively, of the static load-carrying capacity of the beam ($P_{u,exp}$). In the fatigue tests, the specimens were loaded dynamically at a rate of 240 cycles per minute using a sinusoidal waveform until failure, except in the case with $P_{max} = 96.1\%$ of $P_{u,exp}$, when the loading frequency was 60 cycles per minute. During the fatigue tests, strain measurements were taken at the tie plates to check whether they fractured or not. Also, at the end of each fatigue test, the concrete was removed to check for fatigue fracture of the tie plates.

3. FINITE ELEMENT ANALYSIS [5]

3.1 Finite Element Idealization

A nonlinear finite element computer program (WCOMR) [6] was used to analyze the steel-concrete sandwich beams shown in Figs.2 and 3a. The finite element mesh of the beams is shown in Fig.4. Eight-node quadratic elements were used for the concrete and steel elements. Each concrete and steel element contains (3×3) Gauss points. The constitutive models for the concrete and steel elements are as given in references [6] and [7]. Bond elements were added to simulate the shear connectors and the interface between concrete and the lower steel plate. A linear bond stress-slip relationship was adopted as the constitutive law for the bond elements⁷⁾. Prescribed displacements were given at the loading point, as shown in Fig.4.

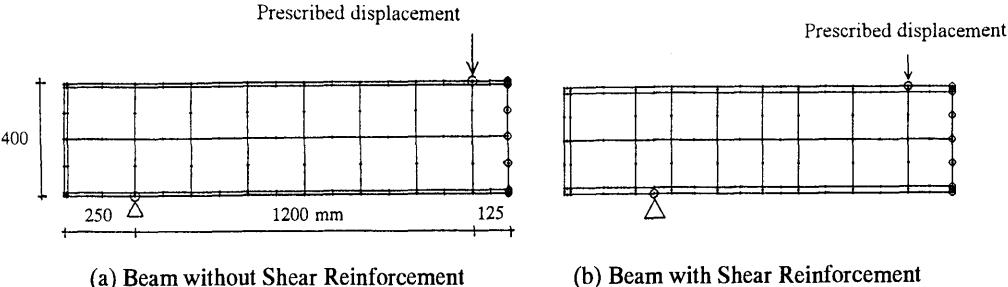


Fig.4 Finite Element Mesh

3.2 Analytical Models For Fatigue

An experimental S-N relationship was adopted as the constitutive law for concrete under fatigue loading.

This $S-N$ relationship is given by the following equation:

$$(f_{max}/f_u) = 1.0 - 0.0685 (1-R) \log N \quad (1)$$

where: f_u = static strength
 $R = f_{min}/f_{max}$ ($0 \leq R \leq 1.0$)
 f_{min} = minimum stress
 f_{max} = maximum stress
 N = number of loading cycles

This $S-N$ relationship was proposed by Tepfers [8][9] to predict the tensile and compressive fatigue strengths of plain concrete. For the applied number of loading cycles (N), Eq.(1) was used to check for tensile and compressive fatigue failure at every concrete Gauss point according to the biaxial stress state at the point. If compressive fatigue failure occurred at one Gauss point, the compressive strength of the point was reduced to the stress at which fatigue failure occurs. Similarly, if tensile fatigue failure occurred at one Gauss point, the tensile strength of the point was reduced.

Previous studies [10][11] have indicated that the secant modulus of elasticity of concrete (E_s) falls during fatigue loading. Therefore, the linear relationship shown in Fig.5 was adopted in this study to model the stiffness degradation of concrete under fatigue loading. This linear relationship is given by the following equation:

$$R_N = 299 - 2.99 (E_f/E_s) \quad (2)$$

where: (E_f/E_s) is given as a percentage
 E_s = modulus of elasticity of the concrete under static loading
 E_f = reduced modulus of elasticity of the concrete under fatigue loading
 R_N = percentage of fatigue life

Therefore, the fatigue analysis was based on reducing the strength and stiffness of the concrete at Gauss points with increasing loading cycles (N) and increasing stress range ($S_r = f_{max} - f_{min}$).

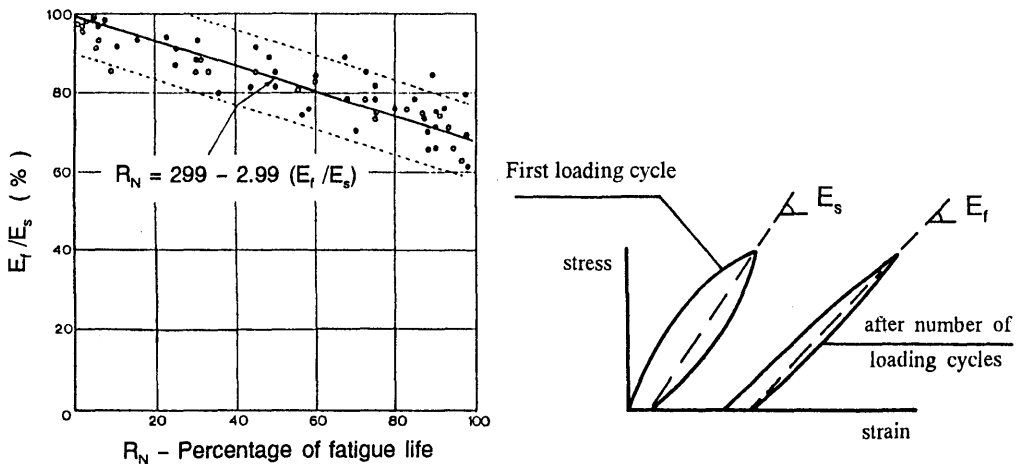


Fig.5 Decrease of Modulus of Elasticity under Repeated Loading[11]

3.3 Analysis Procedure

The analysis procedure used in this study is illustrated in Fig.6. First, a static loading cycle (OAB) is applied. The principal compressive and tensile stresses of every concrete Gauss point at maximum

fatigue load (σ_{cmax} , σ_{tmax}) are stored at point A. Similarly, the principal compressive and tensile stresses of every concrete Gauss point at minimum fatigue load (σ_{cmin} , σ_{tmin}) are stored at point B. Then, these stored principal stresses are used to calculate the mean and deviatoric stresses as shown in Fig.7 [6], hence:

$$\sigma_{m,max} = 2^{1/2} (\sigma_{tmax} + \sigma_{cmax}) / 2 \quad (3)$$

$$\tau_{d,max} = 2^{1/2} (\sigma_{tmax} - \sigma_{cmax}) / 2 \quad (4)$$

similarly:

$$\sigma_{m,min} = 2^{1/2} (\sigma_{tmin} + \sigma_{cmin}) / 2 \quad (5)$$

$$\tau_{d,min} = 2^{1/2} (\sigma_{tmin} - \sigma_{cmin}) / 2 \quad (6)$$

Thereafter, the equivalent stresses at maximum and minimum fatigue loads (S_{max} , S_{min}) are calculated as shown in Fig.8 [6], hence:

$$S_{max} = [(a\sigma_{m,max})^2 + (b\tau_{d,max})^2]^{0.5} \leq 1.0 \quad (7)$$

$$S_{min} = [(a\sigma_{m,min})^2 + (b\tau_{d,min})^2]^{0.5} \leq 1.0 \quad (8)$$

where: $a = 0.6/f_c'$, and $b = 1.3/f_c'$

These equivalent stresses (S_{max} , S_{min}) indicate the level of applied stress at any Gauss point under plane stress. Then, substituting ($f_{max} = S_{max}$), ($f_{min} = S_{min}$), and ($f_u = 1.0$) in Eq.(1), the number of loading cycles (N_C) can be calculated. The number of cycles (N_C) is defined as the number of loading cycles required to induce compression fatigue failure at this particular concrete Gauss point.

The stored principal stresses together with the cracking criterion of concrete are used to calculate stress ratios, (R_{min}) and (R_{max}), as shown in Figs9(a) and 9(b). In Fig.9(a), the point (σ_{tmin} , σ_{cmin}), which indicates the principal stresses at the minimum fatigue load, is plotted, and hence the ratio of principal stress to strength, (R_{min}) is calculated as,

$$R_{min} = \sigma_{tmin} / f_{t1} \leq 1.0 \quad (9)$$

Similarly, in Fig.9(b), the point (σ_{tmax} , σ_{cmax}) is plotted, and hence the ratio (R_{max}) is calculated as,

$$R_{max} = \sigma_{tmax} / f_{t2} \leq 1.0 \quad (10)$$

Then, substituting ($f_{max} = R_{max}$), ($f_{min} = R_{min}$), and ($f_u = 1.0$) in Eq.(1), the number of loading cycles (N_T) can be calculated. The number of cycles (N_T) is defined as the number of loading cycles required to induce tension fatigue failure at this concrete Gauss point.

The input number of cycles (N_I) is compared with the calculated values (N_C and N_T):

- if $N_I \geq N_C$, the concrete Gauss point is considered to fail in compression, and therefore, the compressive strength of this Gauss point is reduced to [$f_c' \times S_{max}$].
- if $N_I \geq N_T$, the concrete Gauss point is considered to fail in tension, and therefore the tensile strength of this Gauss point is reduced to [$f_t \times R_{max}$]. Also, the stiffness of the concrete is reduced to 66% of its initial value. The ratio 66% is the minimum value given by Eq.(2) when ($R_N = 100\%$).
- if $N_I < N_T$, the concrete Gauss point is considered not to have failed in tension yet. In this case, the stiffness of concrete is reduced according to Eq.(2), in which the percentage of fatigue life (R_N) is given by,

$$R_N = (N_I / N_T) \times 100 \quad (11)$$

Thereafter, a second loading cycle (BCD) is applied (see Fig.6). The reduction in concrete tensile strength (f_t) will result in earlier cracking for the concrete Gauss points. If the Gauss point has already cracked, the reduction in f_t will result in a downward shift in the tension stiffening branch of the concrete, as shown in Fig.10. Hence, for the same tensile strain (i.e., crack opening), the tensile force transferred normal to the crack surface will be reduced. The concrete tension stiffening model for fatigue analysis in Fig.10 is given by the following equation:

$$\sigma_t / f_t = \beta (\varepsilon_{tu} / \varepsilon_t)^{0.4} \quad (12)$$

where: σ_t = tensile stress
 ε_t = tensile strain
 f_t = tensile strength of concrete
 $\varepsilon_{tu} = 0.02\%$
 β = reduction factor for fatigue analysis

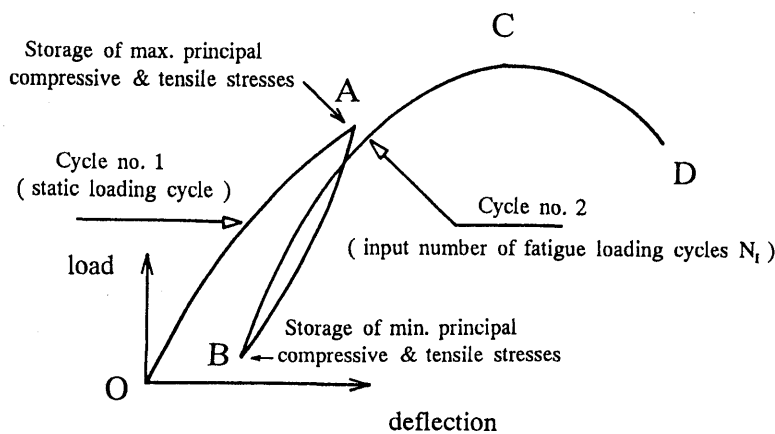


Fig.6 Analysis Procedure

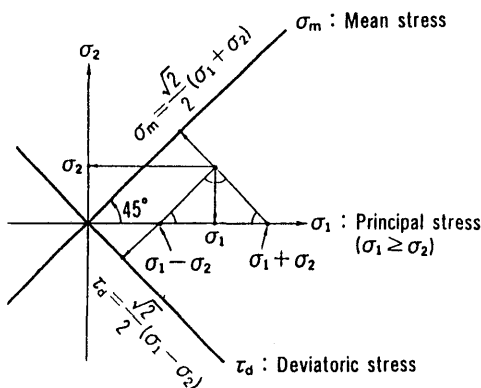


Fig.7 Mean and Deviatoric Stress Coordinator[6]

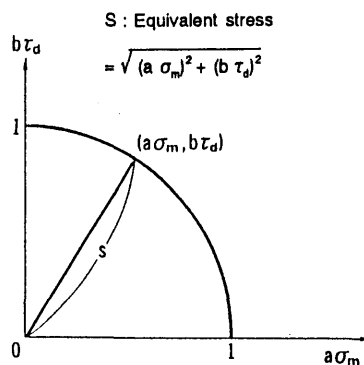


Fig.8 Definition of Equivalent Stress[6]

On the other hand, the reduction in stiffness of uncracked concrete Gauss points (E_c) will weaken the stiffness of the concrete elements. Also, the reduction in concrete stiffness (E_c) results in a lower concrete shear modulus (G_c) which in turn results in a reduced shear force transferred parallel to the crack surface. The reduction in tensile and shear forces transferred at the crack surface might offer a convenient model for simulating the increase in crack width under fatigue loading. Since the effect of the reduction in concrete stiffness due to concrete fatigue in compression was found to be negligible, only the reduction in concrete stiffness due to fatigue of concrete in tension was considered, as described

in the cases of $N_f \geq N_T$ and $N_f < N_T$.

Therefore, during the second loading cycle (BCD) in Fig.6, the strength and stiffness of concrete Gauss points are reduced, which in turn results in a lower overall stiffness of the sandwich beam. Finally, the sandwich beam is considered to fail due to fatigue loading (N_f cycles) if the peak load of the second cycle (point C in Fig.6) is approximately equal to the peak load of the first cycle (point A in Fig.6). In this case, the input number of cycles (N_f) is considered to be equal to the fatigue life of the sandwich beam. Note that, in this study, it is simply assumed that Eq.(1) is applicable to the biaxial state of stresses ((S_{max}, S_{min}) and (R_{max}, R_{min})). Further study is necessary to prove this assumption by fatigue tests on concrete elements under biaxial stress conditions.

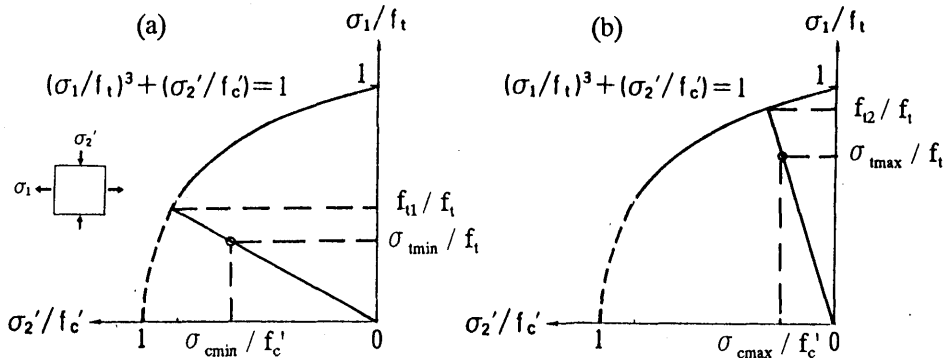


Fig.9 Cracking Criterion for Concrete (Biaxial Tension-Compression)[6]

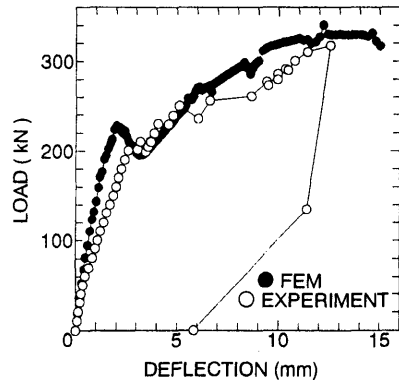
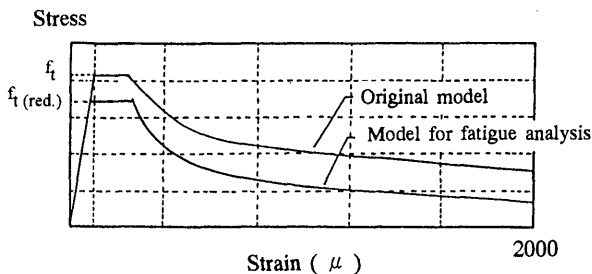


Fig.10 Tension Stiffening Model for Fatigue Analysis Fig.11 Load-Deflection Curves under Static Loading

4. RESULTS AND DISCUSSION

4.1 Sandwich Beams Without Shear Reinforcement

(1) Static Monotonic Loading

As described, a sandwich beam (specimen 1) was first tested under static monotonic loading. The beam was also numerically analyzed under static monotonic loading using the finite element method. The experimental and numerical load-deflection curves are shown in Fig.11. It can be seen that stiffness remains high until a load of about 230 kN. At this point, main diagonal cracking occurs in both experiment and analysis. This is illustrated by the crack pattern shown in Fig.12. Thereafter the deflection increases with decreased stiffness until the ultimate failure load. The experimental ultimate failure load ($P_{u,exp}$) was 318 kN, while the analytical ultimate failure load ($P_{u,FEM}$) was equal to 340 kN. In both experiment and numerical analysis, the beam failed in shear compression mode. This failure

mode is characterized by diagonal cracking and concrete crushing, as shown in Fig.12.

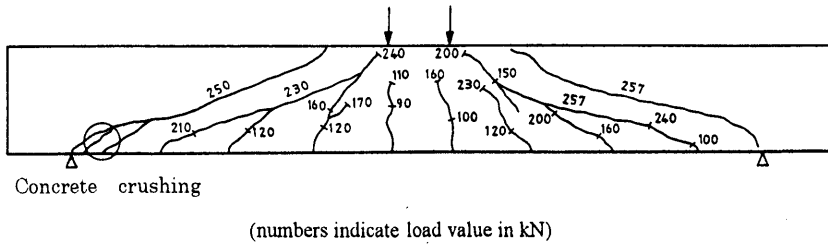


Fig.12 Crack Pattern under Static Monotonic Loading

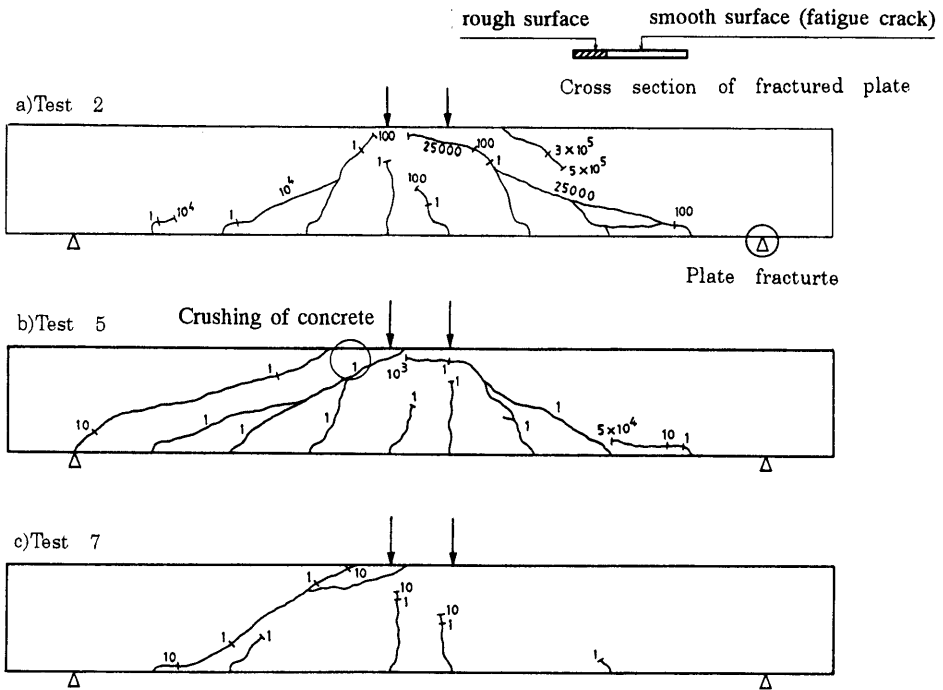


Fig.13 Crack Patterns and Failure Modes under Fatigue Loading

(2) Fatigue Loading

a) Results of fatigue tests

Eight fatigue tests were carried out. The results are illustrated in Table 1. The crack patterns of the sandwich beam specimens in fatigue tests 2, 5, and 7 are shown in Fig.13. The numbers given on the crack patterns indicate the number of fatigue loading cycles (N). In fatigue test 1 ($P_{max} = 38.7\%$ of $P_{u,exp}$), fatigue failure did not occur until 10×10^6 cycles. In fatigue test 2 ($P_{max} = 49.0\%$ of $P_{u,exp}$) and 3 ($P_{max} = 63.2\%$ of $P_{u,exp}$), fatigue failure occurred due to fracturing of the tensile steel plate at the support point (see Fig.13a). In fatigue tests 2 and 3, after the development of the main diagonal cracks, the section of the lower steel plate between the support and the second outer shear connector was subjected to local bending deformation because of the restraint provided by the support. Also, the greatest slip between concrete and lower steel plate was observed in this section. Thereafter, the steel plate fractured at the support point, which was a weak point since the shear connector was welded to the plate and local bending deformation caused local bending stresses. A cross section of the steel plate at the fracture point is shown at top of Fig.13a, in which the white area indicates the fatigue crack, while the hatched area indicates the part that finally fractured in tension after the growing fatigue crack weakened the plate. In fatigue tests 4 ($P_{max} = 65.5\%$ of $P_{u,exp}$), 5 ($P_{max} = 70.7\%$ of $P_{u,exp}$), and 6

($P_{max} = 82.1\%$ of $P_{u,exp}$), fatigue failure occurred due to crushing of concrete between the diagonal cracks (see Fig.13b). In fatigue test 7 ($P_{max} = 43.1\%$ of $P_{u,exp}$), fatigue failure occurred after 20 cycles and the failure mode was a diagonal tension failure (see Fig.13c). In fatigue test 8 ($P_{max} = 58.5\%$ of $P_{u,exp}$), the maximum load was designed to be 76% of $P_{u,exp}$ but in the actual test the sandwich beam failed at 185 kN (i.e., 58.5% of $P_{u,exp}$) in the first loading cycle. The failure mode was diagonal tension failure. In fatigue tests 7 and 8, the sandwich beam failed due to propagation of a main diagonal crack without any crushing of the core concrete, as shown in Fig.13c. This failure mode is different from the one described in Section 4.1(1). The experimental S-N relationship of the sandwich beam is shown in Fig.14. More details of these the experimental results can be found in reference [4].

Table 1 Results of Fatigue Tests on Beams without Shear Reinforcement

Specimen No.	Fatigue test No.	$P_{max} / P_{u,exp}$ (%)	Fatigue life (cycles)	Failure mode
2	1	38.7	2,000,000	NF ¹⁾
3	2	49.0	624,221	FS ²⁾
4	3	63.2	120,081	FS ²⁾
2	4	65.5	79,948	SC ³⁾
5	5	70.7	50,983	SC ³⁾
6	6	82.1	11	SC ³⁾
7	7	43.1	20	DT ⁴⁾
8	8	58.5	1	DT ⁴⁾

- 1) NF : no fatigue failure up to 2,000,000 cycles
- 2) FS : fracture of the lower steel plate at the support point (see Fig.13a)
- 3) SC : shear compression failure (crushing of concrete between the diagonal cracks)(see Fig.13b)
- 4) DT : diagonal tension failure (propagation of main diagonal crack without any crushing of the core concrete) (see Fig.13c)

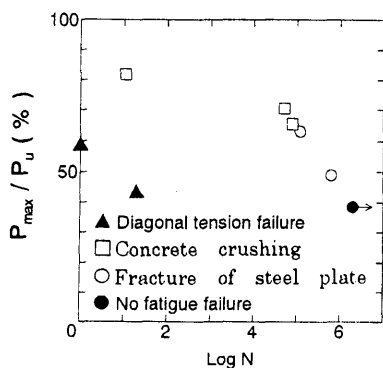


Fig.14 Experimental S-N Relationship of Sandwich Beam

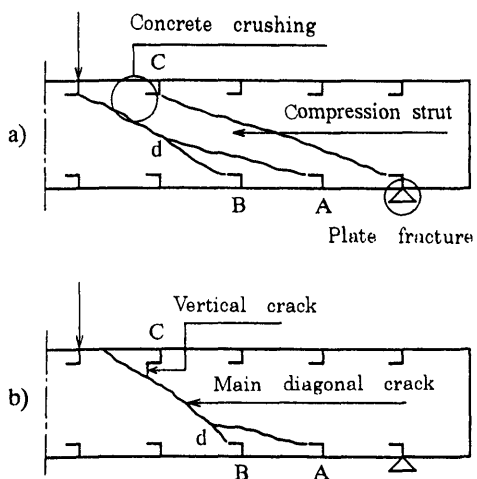


Fig.15 Effect of Crack Pattern on Failure Mode of Sandwich Beam

Figure 15 illustrates how the crack pattern affects the failure mode of the sandwich beam. In Fig.15a, diagonal cracks originate from the shear connectors (A) and (B) at the bottom fiber of the sandwich beam. These two diagonal cracks come together at point (d) and then propagate as a single crack at an angle of about 30° towards the loading point. Thereafter, another diagonal crack originates from shear connector (C) at the top fiber of the beam, and this crack propagates downward towards the support

point. Therefore, the tied-arch mechanism comes into play and finally the sandwich beam fails either by crushing of the concrete compression strut or by fracture of the steel plate at the support point. In Fig.15b, the diagonal cracks from the shear connectors (A) and (B) converge at point (d) and then propagate at about 40° towards the loading point. In this case, the crack path passes close to the shear connector (C). As a result, a vertical crack occurs between shear connector (C) and the main diagonal crack (see Fig.15b). In this case, the tied-arch mechanism does not operate, and diagonal tension failure occurs. It is notable that the diagonal cracks originate at the locations of shear connectors and then propagate with increasing loading cycles (N). Therefore, it can be said that the arrangement of shear connectors affects the failure mode of the sandwich beam.

b) Results of fatigue analysis

The fatigue strength of a sandwich beam suffering failure due to concrete crushing was predicted using the finite element method. The sandwich beam was analyzed for different external load ranges. The minimum fatigue load (P_{min}) was kept constant at 20 kN. The maximum fatigue load (P_{max}) was chosen to be 240 kN, 270 kN, and 300 kN which is 70.6%, 79.4%, and 88.2%, respectively, of the analytical static strength of the beam ($P_{u,FEM} = 340$ kN). The analytical results are summarized in Table 2. The output load-deflection curves for beams 2 and 3 are shown in Fig.16. Note that the overall stiffness of these beams falls in the second and third loading cycles because of increasing the crack propagation, and the beam finally fails due to concrete crushing at the maximum fatigue load. The analytical $S-N$ relationship of this sandwich beam is shown in Fig.17a, along with the experimental relationship for the same failure mode (i.e., concrete crushing failure mode). Good agreement is apparent between the experimental and the analytical $S-N$ relationships.

Table 2 Results of Fatigue Analysis (Failure by Concrete Crushing)

Beam	P_{min} (kN)	P_{max} (kN)	$P_{max} / P_{u,exp}$ (%)	Fatigue life (cycles)	Failure mode
1	20	240	70.6	20,000	SC ¹⁾
2	20	270	79.4	1,000	SC ¹⁾
3	20	300	88.2	50	SC ¹⁾

1) SC : shear compression failure (crushing of core concrete)

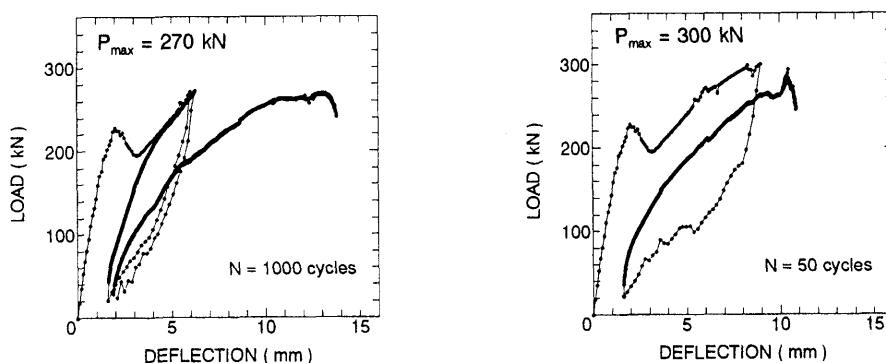


Fig.16 Analytical Load-Deflection Curves

Next, a sensitivity analysis was carried out to clarify the effect of a reduction in each of four factors, i.e., compressive strength (f_c'), tensile strength (f_t), concrete stiffness (E_c), and shear modulus (G_c) on the fatigue strength of the sandwich beam. The analysis was carried out for the beam 2 in Table 2. This analysis indicated that a reduction in no single factor could fully explain the strength reduction due to

fatigue. Some factors affected the fatigue strength more significantly than others did. A comparison of predicted fatigue lives with reductions in different combinations of factors is shown in Table 3. If a reduction is made in all factors (f_c', f_t, E_c, G_c), the fatigue life of the beam is 1,000 cycles. The most influential factor on the fatigue life of the beam is the tensile strength of concrete (f_t) because if (f_t) is kept constant and a reduction is made in all other factors (f_c', E_c, G_c), the fatigue life of the beam increases to 1,200 cycles. The shear modulus (G_c) also has some effect on the fatigue life of the beam, because when (G_c) is kept constant and a reduction is made in (f_c', f_t, E_c), the fatigue life of the beam increases to 1,100 cycles. However, when the concrete compressive strength (f_c') is kept constant and when the concrete stiffness (E_c) is kept constant, the fatigue life of the beam remains the same, as shown in Table 3. Thus the analysis indicates that the most influential factor is the concrete tensile strength (f_t), followed by the shear modulus at crack (G_c), then the concrete stiffness (E_c), and lastly the compressive strength (f_c'). It can be said from this analysis that crack propagation and the increase in shear deformation due to the reduction of these factors causes earlier shear compression failure under fatigue loading.

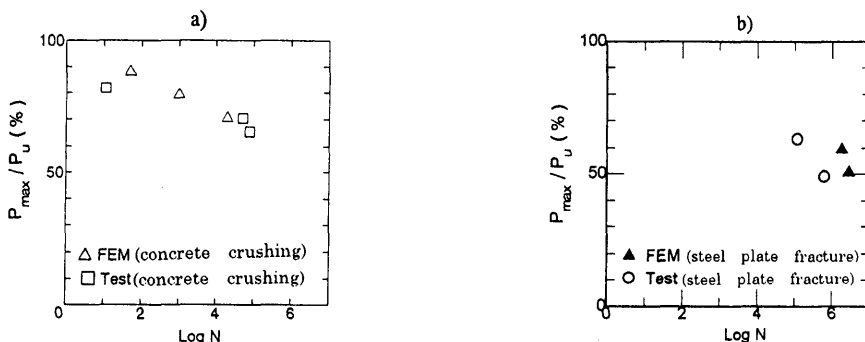


Fig.17 Comparison between Experimental and Analytical S-N Relationships

Table 3 Results of Sensitivity Fatigue Analysis

	Reduction of (f_c', f_t, E_c, G_c)	Reduction of (f_t, E_c, G_c) only	Reduction of (f_c', E_c, G_c) only	Reduction of (f_c', f_t, G_c) only	Reduction of (f_c', f_t, E_c) only
Fatigue life (cycles)	1000	1000	1200	1000	1100

The fatigue strength of a sandwich beam suffering failure by fracture of the steel plate was also predicted using the finite element method. In this case, the sandwich beam was analyzed for two different external load ranges. The minimum fatigue load (P_{min}) was kept constant at 20 kN. The maximum fatigue load (P_{max}) was chosen to be 50.7% and 59.6% of the analytical static strength of the beam ($P_{u,FEM} = 340$ kN). The fatigue analysis was carried out using the following procedure:

- First, a static loading cycle (OAB) was applied as shown in Fig.6.
- The maximum tensile stress in the lower steel plate at the location of the second outer shear connector was stored at point (A). Similarly, the minimum tensile stress in the lower steel plate at the location of the second outer shear connector was stored at point (B). Hence, the stress range in the lower steel plate at the location of the second outer shear connector was calculated. This location was selected because the strains in the lower steel plate at this point were recorded in fatigue test 2 (see Table 1). Consequently, it is possible to estimate the additional stresses induced in the steel plate due to local bending deformations as well as the additional stresses due to the shear transfer between the concrete and the lower steel plate. Unfortunately, the strain measurements at the actual fracture point (i.e., the support point) were not available and so the location of the second outer shear connector was selected.
- Next, the calculated stress range was multiplied by an amplification factor to account for the effect of local bending deformations of the steel plate as well as the effect of the shear transfer between the concrete and the lower steel plate. In this study, the amplification factor was approximately 5.0, and was obtained by comparing the stress range of the steel plate measured in fatigue test 2 (see Table 1) with the

stress range measured in a fatigue test in air [12].

- Then, using the S_r - N relationship of the steel plate in air⁽²⁾ and knowing the value of the amplified stress range, the number of loading cycles (N_F) was calculated as shown in Fig.18.

- If the input number of cycles (N_I) was equal to the calculated value (N_F), the sandwich beam was considered to fail due to fracture of the lower steel plate after the loading cycles (N_I).

The analytical results are summarized in Table 4. The analytical S - N relationship of the sandwich beam is shown in Fig.17b, and also compared with the experimental relationship for the same failure mode (i.e., steel plate fracture).

Table 4 Results of Fatigue Analysis (Failure by Steel Plate Fracture)

Beam	P_{min} (kN)	P_{max} (kN)	$P_{max} / P_{u,FEM}$ (%)	Fatigue life (cycles)	Failure mode
1	20	172	50.7	2,735,000	FS ¹⁾
2	20	203	59.6	1,820,000	FS ¹⁾

1) FS : fracture of the lower steel plate

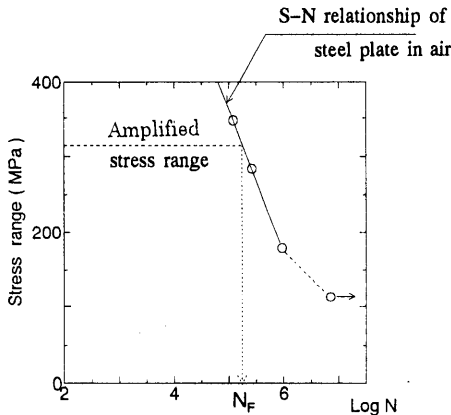


Fig.18 Prediction of Fatigue Life of Beam which Fails due to Fracture of Steel Plate

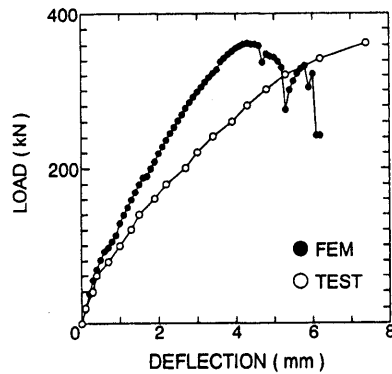


Fig.19 Load-Deflection Curves under Static Loading

4.2 Sandwich Beams With Shear Reinforcement

(1) Static Monotonic Loading

First, sandwich beam (specimen A1) was tested under static monotonic loading. The beam was also subject to numerical analysis under static monotonic loading using the finite element method. The experimental and analytical load-deflection curves are shown in Fig.19. The experimental ultimate failure load ($P_{u,exp}$) was 362.7 kN, while the analytical ultimate failure load ($P_{u,FEM}$) was equal to 362.5 kN. In both experiment and analysis, the failure mode of the beam was shear compression failure characterized by diagonal cracking and concrete crushing, as shown in Fig.20. There is excellent agreement between the analytical and experimental ultimate failure loads, as indicated by Fig.19. However, the analytical load-deflection curve indicates a higher stiffness than the experimental one, a difference that may result from an overestimation of the stiffness of the bond elements. Unfortunately, there is no available experimental data from which the stiffness of the bond elements could be estimated precisely. Furthermore, some instability was observed in the analytical load-deflection curve once the concrete in some elements enters the softening range, as also shown in Fig.19.

(2) Fatigue Loading

a) Results of fatigue tests

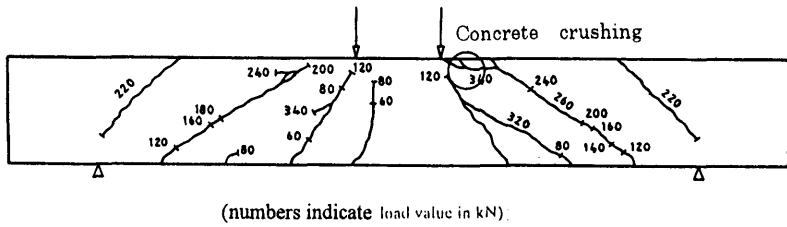


Fig.20 Crack Pattern under Static Monotonic Loading

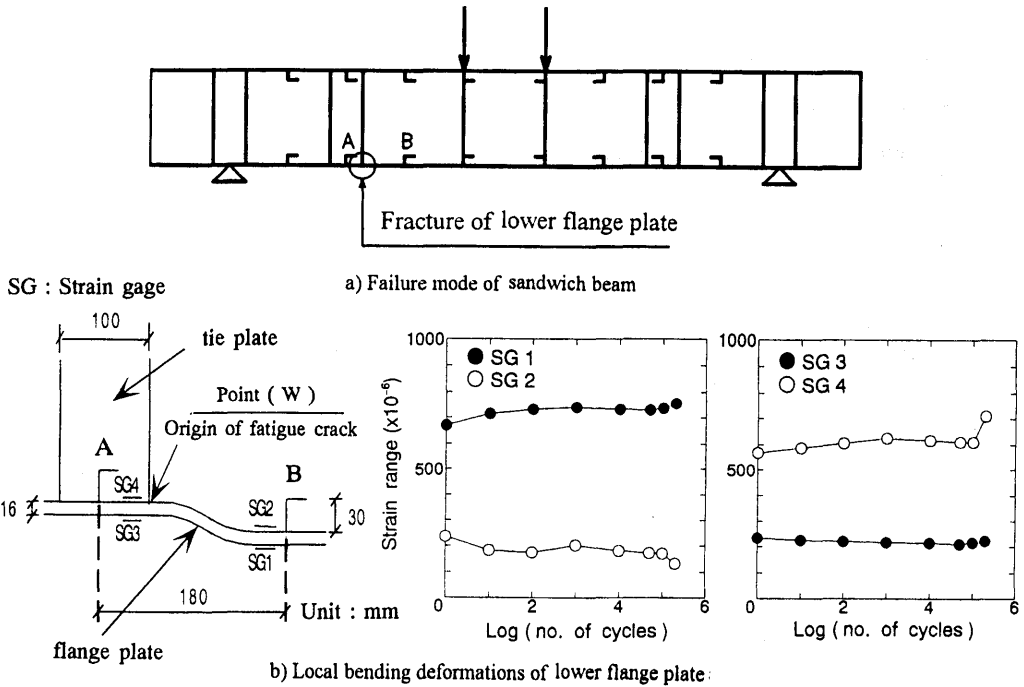


Fig.21 Failure Mode in Fatigue Test 1 ($P_{max} / P_u = 52.5\%$)

Fatigue tests were carried out for five sandwich beams of type A (specimens A2, A3, A4, A5, and A6). For these specimens, the maximum fatigue load (P_{max}) was 52.5%, 68.3%, 81.1%, 90.4%, and 96.1%, respectively, of the experimental static strength of the beam ($P_{u,exp}$). The results of the fatigue tests are illustrated in Table 5. In fatigue test 1 ($P_{max} = 52.5\%$ of $P_{u,exp}$), fatigue failure occurred due to fracture of the lower flange plate, as shown in Fig.21a. The strain measurements indicate that section AB of the lower flange plate was subjected to local bending deformations (see Figs.21a and 21b). These local bending deformations result in a concentration of tensile stresses at point W, which is the edge of the weld line between the tie plate and the lower flange plate (see Fig.21b). Therefore, a fatigue crack originated at point W and propagated through the lower flange plate with increasing loading cycles (N) until complete fracture occurred. In fatigue test 2 ($P_{max} = 68.3\%$ of $P_{u,exp}$), the sandwich beam failed due to concrete crushing in the vicinity of the loading point, as shown in Fig.22a. Thereafter, the concrete was removed and a 50 mm fatigue crack was found to have propagated in the tie plate (see Fig.22b). In fatigue test 3 ($P_{max} = 81.1\%$ of $P_{u,exp}$), the sandwich beam failed due to concrete crushing in the vicinity of the loading point, as shown in Fig.22a. The concrete was removed and the tie plate was found to have completely fractured (i.e., completely separated from the lower flange plate) (see Fig.22c). In fatigue

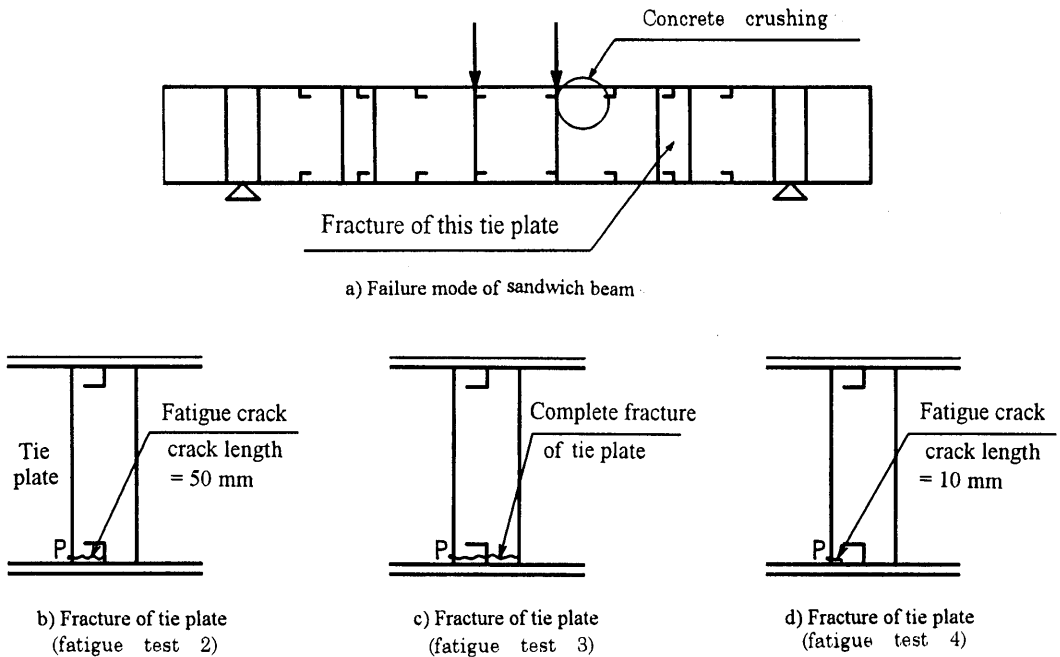


Fig.22 Failure Mode in Fatigue Tests 2, 3 and 4

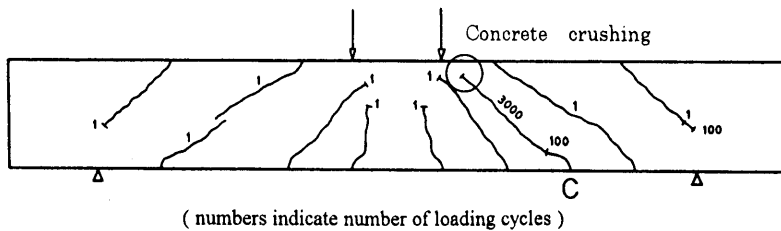


Fig.23 Crack Pattern of Sandwich Beam in Fatigue Test 3

test 4, the sandwich beam was subjected to 6,000 cycles during which the fatigue load fluctuated between a minimum value of $P_{min} = 14.3\%$ of $P_{u,exp}$ and a maximum value of $P_{max} = 86\%$ of $P_{u,exp}$. Thereafter, the load range was widened to range between a minimum value of $P_{min} = 5.5\%$ of $P_{u,exp}$ and a maximum value of $P_{max} = 90.4\%$ of $P_{u,exp}$. Fatigue failure occurred after 2,100 cycles at the higher load range (i.e., $P_{min} = 5.5\%$ and $P_{max} = 90.4\%$ of $P_{u,exp}$). In this test, the sandwich beam failed due to concrete crushing in the vicinity of the loading point, as shown in Fig.22a. The concrete was removed and a fatigue crack of 10 mm in length was found to have propagated in the tie plate (see Fig.22d). In fatigue tests 2, 3, and 4, the failure mode of the sandwich beam is considered to be fracture of the tie plate. That occurred because the fatigue crack appeared in the tie plate at first, and then a new diagonal crack originated from the shear connector at point C (see Fig.23) and propagated towards the loading point. This leads to increased deflection of the beam and finally concrete crushing takes place. It is observed that the tie plate fractures always occur at the welds between tie plate and lower flange plate. Also, the fatigue crack always starts at point P, which is the most tensioned point in the tie plate (see Figs.22b, 22c, and 22d). This can be illustrated by the relationship between the number of loading cycles (N) and the strain range in the tie plate, as shown in Fig.24 In fatigue test 5 ($P_{max} = 96.1\%$ of $P_{u,exp}$), the sandwich beam failed due to concrete crushing in the vicinity of the loading point. The concrete was removed after

the test and the tie plate was found to be sound (i.e., no fatigue crack had occurred in the tie plate). Therefore, in this fatigue test, the failure mode of the beam was considered to be concrete crushing. The $S-N$ relationship for fatigue failure of sandwich beams of type A is shown in Fig.25. Note that the fatigue life of the beam at $P_{max}/P_{u,exp} = 90.4\%$ is plotted as two points connected by a dotted line, the first point at 2,100 cycles and the second point at 8,100 cycles. The first point neglects the effect of the 6,000 cycles with $P_{max}=86\%$ of $P_{u,exp}$ and $P_{min}=14.3\%$ of $P_{u,exp}$. On the other hand, the second point considers the effect of the small load range ($P_{max}=86\%$ and $P_{min}=14.3\%$ of $P_{u,exp}$) in exactly the same way as the effect of the larger load range ($P_{max}=90.4\%$ and $P_{min}=5.5\%$ of $P_{u,exp}$). Hence, the fatigue life of the beam is actually located somewhere between 2,100 cycles and 8,100 cycles.

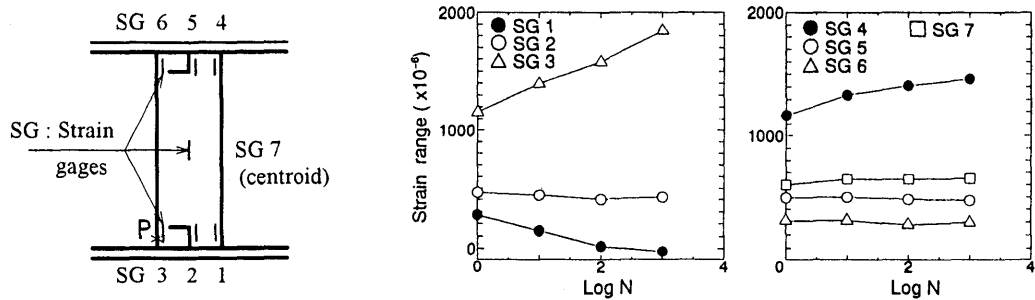


Fig.24 Relationship between $\log N$ and Strain Range in the Fractured Tie Plate in Fatigue Test 3

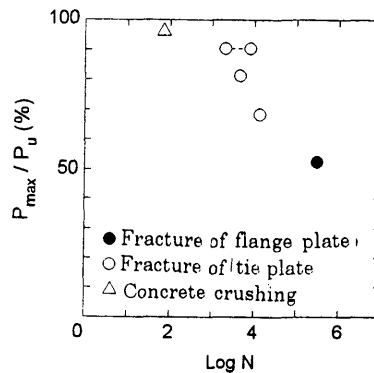


Fig.25 $S-N$ Relationship of Beam Type A

Table 5 Results of fatigue tests on beams with shear reinforcement

Fatigue test	Specimen	$P_{min} / P_{u,exp}$ (%)	$P_{max} / P_{u,exp}$ (%)	Fatigue life (cycles)	Failure mode
1	A2	5.5	52.5	310,799	FP ¹⁾
2	A3	5.5	68.3	13,724	TP ²⁾
3	A4	5.5	81.1	4662	TP ²⁾
4	A5	14.3	86.0	6000	TP ²⁾
		5.5	90.4	2100	
5	A6	5.5	96.1	70	CC ³⁾
6	B1	5.5	54.3	51,389	TP ²⁾
7	B2	5.5	41.8	526,000	TP ²⁾

1) FP : Fracture of lower flange plate 2) TP : Fracture of tie plate 3) CC : Concrete crushing

Fatigue tests were carried out for two sandwich beams of type B (specimens B1 and B2). The maximum

fatigue load (P_{max}) was equal to 54.3% and 41.8%, respectively, of the experimental static strength of the beam ($P_{u,exp}$). The results of these fatigue tests are illustrated in Table 5. In fatigue test 6 ($P_{max} = 54.3\%$ of $P_{u,exp}$), the sandwich beam failed due to concrete crushing in the vicinity of the loading point, as shown in Fig.26. The fatigue life of the beam was equal to 51,389 cycles. The failure occurred in the shear span in which the tie plates were placed parallel to the member axis (see Fig.26). After the test, the concrete was removed and the middle and outer tie plates were found to be completely fractured (i.e., completely separated from the lower flange plate), as shown in Fig.26. Also, the outer shear connector was completely separated from the lower flange plate (see Fig.26). The strain measurements indicated that the middle tie plate fractured between 10^4 cycles and 5×10^4 cycles (because the maximum strain of the middle tie plate dropped suddenly between 10^4 cycles and 5×10^4 cycles, while the maximum strains of the inner and the outer tie plates increased (see Fig.26)). Hence, the contribution of the inner and outer tie plates increases after fracturing of the middle tie plate. Although the middle tie plate fractured, the sandwich beam was still able to sustain the maximum load and the fatigue test continued until 51,389 cycles. At 51,389 cycles, the outer tie plate fractured and concrete crushing occurred. In fatigue test 7 ($P_{max}=41.8\%$ of $P_{u,exp}$), the sandwich beam failed due to concrete crushing in the vicinity of the loading point as shown in Fig.27. The fatigue life of the beam was 526,000 cycles. Failure occurred in the shear span in which the tie plates were placed normal to the member axis (see Fig.27). After the test, the concrete was removed and all three tie plates were found to have fractured, as shown in Fig.27.

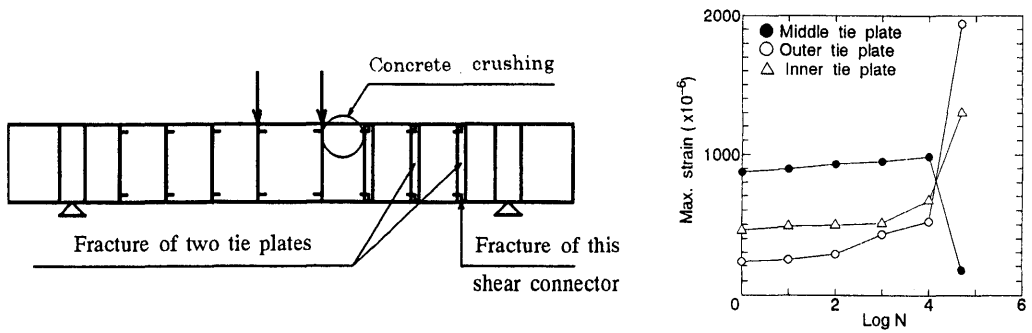


Fig.26 Failure Mode in Fatigue Test 6 ($P_{max} / P_{u,exp} = 54.3\%$)

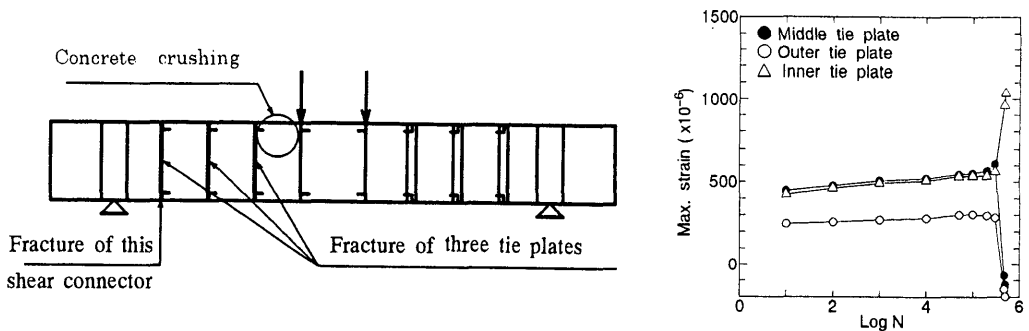


Fig.27 Failure Mode in Fatigue Test 7 ($P_{max} / P_{u,exp} = 41.8\%$)

The middle and outer tie plates were completely separated from the lower flange plate, while the inner tie plate was completely separated from the upper flange plate. Also, the outer shear connector was completely separated from the lower flange plate (see Fig.27). Strain measurements indicated that the middle and outer tie plates fractured between 300,000 cycles and 482,000 cycles (because the maximum strains of the middle and outer tie plates dropped suddenly between 300,000 cycles and 482,000 cycles, while the maximum strain of the inner tie plate increased (see Fig.27)). Hence, the contribution of the inner tie plate increases after fracturing of the middle and outer tie plates. Although the middle and outer tie plates fractured, the sandwich beam was still able to sustain the maximum load, and the fatigue test continued until 526,000 cycles. At 526,000 cycles, the inner tie plate fractured and concrete crushing occurred. In fatigue tests 6 and 7, the failure mode of the sandwich beam was considered to be fracture

of the tie plates. This is because fracturing of the tie plates occurred first followed by concrete crushing. Note that fracture of the tie plates occurs always at the welds between the tie plate and the flange plate. The $S-N$ relationship for fatigue failure of sandwich beams of type B is shown in Fig.28.

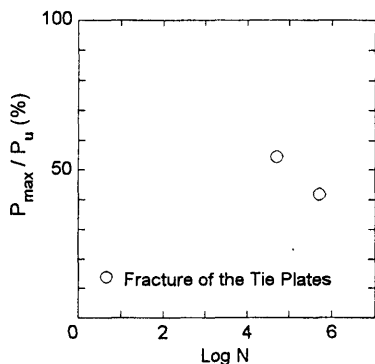


Fig.28 S-N Relationship of Beam Type B

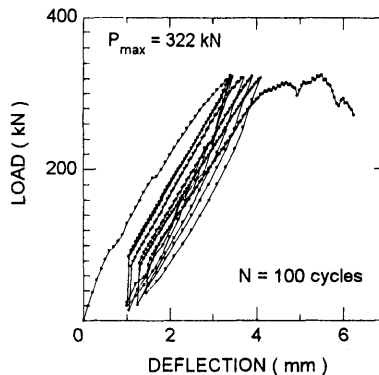


Fig.29 Analytical Load-Deflection Curve

b) Results of fatigue analysis

The fatigue strength of sandwich beams suffering failure due to concrete crushing was predicted using the finite element method. The analytical models used for fatigue analysis as well as the analysis procedure are explained in detail in reference 2). The fatigue analysis was based on reducing the compressive strength (f'_c), tensile strength (f_t), and stiffness (E_c) of the concrete stiffness with increasing loading cycles (N) or increasing concrete stress range (S_r). Analysis was carried out for two different external load ranges. The minimum fatigue load (P_{min}) was kept constant at 20 kN. The maximum fatigue load (P_{max}) was chosen to be 290 kN and 322 kN, which is 80.0% and 88.8%, respectively, of the analytical static strength of the beam ($P_{u,FEM}=362.5$ kN). The analytical results are illustrated by beams 1 and 2 in Table 6. The output load-deflection curve for beam 2 is shown in Fig.29. As shown in Fig.29, the beam was loaded until the maximum fatigue load (P_{max}) and then unloaded until the minimum fatigue load (P_{min}) in order to calculate the maximum and minimum stresses at every concrete Gauss point. The maximum and minimum stresses at every concrete Gauss point were updated as the crack propagation progresses. These maximum and minimum stresses were used together with the input number of loading cycles ($N=100$ cycles) to adjust the strength and stiffness at the concrete Gauss points downward. The reduction in the strength and stiffness at the concrete Gauss points results in a lower overall stiffness of the beam and finally to failure of the beam by concrete crushing at the maximum fatigue load, as shown in Fig.29. Some instability was observed in the analytical load-deflection curve once the concrete in some elements entered the softening range, as shown in Fig.29. Hence, for a percentage of $P_{max}/P_{u,FEM}=88.8\%$, the fatigue life of the beam was considered to be 100 cycles. The analytical $S-N$ relationship of the sandwich beam is shown in Fig.30a, and also compared with the experimental relationship for the same failure mode (i.e., concrete crushing failure mode).

The fatigue strength of a sandwich beam with failure due to fracture of the flange plate was also predicted using the finite element method. The sandwich beam was analyzed for different external load ranges. The minimum fatigue load (P_{min}) was kept constant at 20 kN. The maximum fatigue load (P_{max}) was chosen to be 55.1%, 69.3%, and 79.6% of the analytical static strength of the beam ($P_{u,FEM}=362.5$ kN). The analysis was carried out using the following procedure:

- First, a static loading cycle (OAB) was applied as shown in Fig.31.
- The maximum tensile stress in the lower flange plate at the critical point was stored at point (A). Similarly, the minimum tensile stress in the lower flange plate at the critical point was stored at point (B). From these results, the stress range in the lower flange plate at the critical point was calculated. In this case, the critical point is the location of the flange plate fracture in the fatigue test (see Fig.21).
- Next, the calculated stress range is multiplied by an amplification factor to account for the effect of local bending deformations of the flange plate as well as the effect of shear transfer between the concrete and the lower flange plate. Unfortunately, the strain measurements right at the fracture point were not available, so the value of the amplification factor could not be calculated precisely. Therefore, the amplification factor was calculated by comparing the stress range of the flange plate calculated by the

finite element method with the stress range measured in a fatigue test in air [12]. This amplification factor was 3.6.

- Using the S_r-N relationship of the flange plate in air¹²⁾ and knowing the value of the amplified stress range, the number of loading cycles (N_f) was calculated as shown in Fig.32.

- If the input number of loading cycles (N_i) (see Fig.31) was equal to the calculated value (N_f), the sandwich beam was considered to fail due to fracture of the lower flange plate after the input number of loading cycles (N_i).

Fig.31 Analysis Procedure

The analytical results are illustrated by beams 6, 7, and 8 in Table 6. The analytical $S-N$ relationship of the beam is shown in Fig.30b, along with the experimental relationship for the same failure mode (i.e., failure due to fracture of flange plate). Excellent agreement is observed between the experimental and analytical results.

Table 6 Results of fatigue analysis

Beam	P_{min} (kN)	P_{max} (kN)	$P_{max} / P_{u,FEM}$ (%)	Fatigue life (cycles)	Failure mode
1	20	290	80.0	1000	CC ¹⁾
2	20	322	88.8	100	CC ¹⁾
3	20	200	55.1	939,000	TP ²⁾
4	20	251.2	69.3	241,300	TP ²⁾
5	20	288.6	79.6	221,000	TP ²⁾
6	20	200	55.1	293,600	FP ³⁾
7	20	251.2	69.3	86,300	FP ³⁾
8	20	288.6	79.6	50,100	FP ³⁾

1) CC : Concrete crushing 2) TP : Fracture of tie plate 3) FP : Fracture of lower flange plate

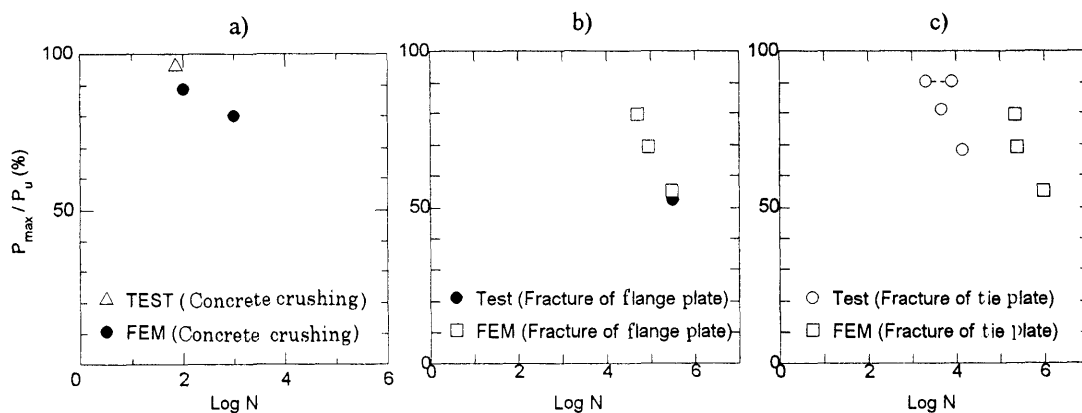


Fig.30 Comparison between Experimental and Analytical $S-N$ Relationships

The fatigue strength of a sandwich beam with failure due to fracture of tie plate was also predicted by using the finite element method. The sandwich beam was analyzed for different external load ranges. The minimum fatigue load (P_{min}) was kept constant at 20 kN. The maximum fatigue load (P_{max}) was chosen to be 55.1%, 69.3%, and 79.6% of the analytical static strength of the beam ($P_{u,FEM}=362.5$ kN). The analysis procedure used was similar to that explained above for predicting failure due to fracture of the flange plate. However, the stress range was calculated at the centroid of the tie plate in this case, and then multiplied by an amplification factor to account for the effect of shear deformations of the tie plates (see Fig.24). In this study, the amplification factor was equal to 3.0. This amplification factor was

obtained by comparing the stress range at the centroid of the tie plate measured in fatigue tests 2, 3, and 4 (see Table 5) with the stress range measured in a fatigue test in air¹³). Then, using the S_r - N relationship of the tie plate in air¹³), the number of loading cycles (N_f) was calculated as shown in Fig.33. If the input number of loading cycles (N_f) was equal to the calculated value (N_f), the beam was considered to fail due to fracture of the tie plate.

The analytical results are illustrated by beams 3, 4, and 5 in Table 6. The analytical S - N relationship of the sandwich beam is shown in Fig.30c, and with the experimental relationship for the same failure mode (i.e., failure due to fracture of tie plate) also shown for comparison. Poor agreement is apparent between the experimental and analytical results. Thus, although the maximum stresses of the tie plates could be predicted reasonably by the finite element method, the minimum stresses and stress ranges could not. Therefore, the predicted fatigue life of the beam is longer than the actual experimental life.

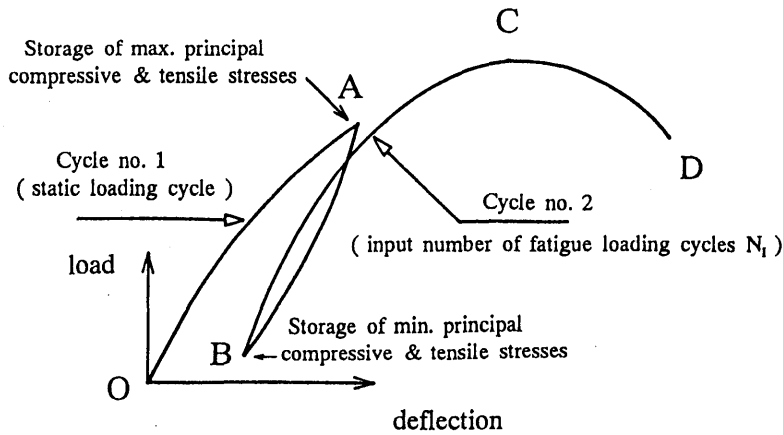


Fig.31 Analysis Procedure

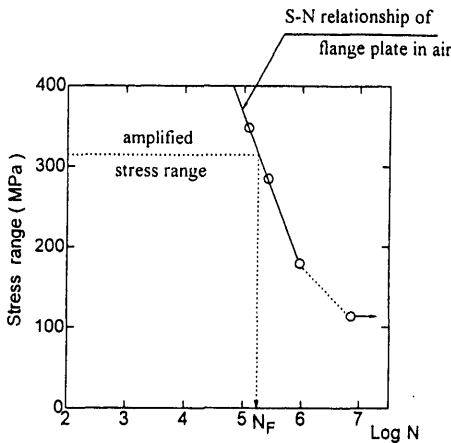


Fig.32 Prediction of Fatigue Life of the Beam which Fails due to Fracture of Flange Plate

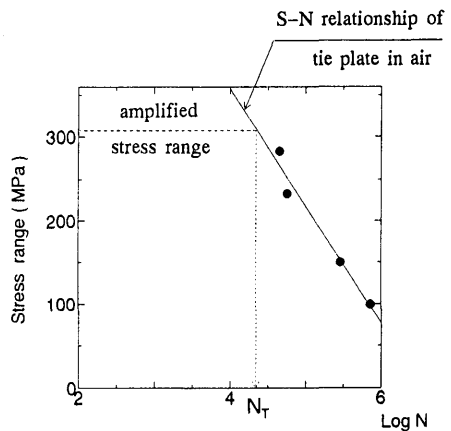


Fig.33 Prediction of Fatigue Life of Beam which Fails due to Fracture of Tie Plate

5. SIMPLE METHOD OF PREDICTING TIE PLATES STRAINS IN SANDWICH BEAMS UNDER FATIGUE LOADING

One of the major aims of this study is to propose a method of predicting the strains in tie plates of sandwich beams under fatigue loading. Studying the shear-fatigue behavior of reinforced concrete

beams, Ueda and Okamura [14] proposed a method of calculating the strains in stirrups under fatigue loading. This method can be used to calculate the maximum strain in the stirrups (i.e., the strain at maximum fatigue load), as well as the strain range. In this study, the same method is used to calculate the strains in the tie plates of sandwich beam shown in Fig.3a. According to this method, the strain in a tie plate at the applied maximum shear force is calculated by the following equation:

$$\varepsilon_{wmax} = \frac{(V_{max} - V_{co}) \times 10^{-0.036(1-r)|\log N}}{A_w E_w} \quad (13)$$

Also, the strain range in the tie plate is calculated by the following equation:

$$\varepsilon_{wr} = \varepsilon_{wmax} (V_{max} - V_{min}) / (V_{max} + V_{co}) \quad (14)$$

where: ε_{wmax} : strain at the centroid of the tie plate at the applied maximum shear force
 ε_{wr} : strain range at the centroid of the tie plate
 V_{max} : applied maximum shear force
 V_{min} : applied minimum shear force
 $r = V_{min} / V_{max}$
 N : number of fatigue loading cycles
 A_w : cross-sectional area of the tie plate
 E_w : modulus of elasticity of the tie plate

The value V_{co} in Eqs.(13) and (14) is the shear force carried by the concrete at initial loading (i.e., in the first loading cycle of the fatigue test). In the case of reinforced concrete beams, the value of V_{co} can be calculated using the following equation [14]:

$$V_{co} = 0.2 f_c'^{1/3} (1 + \beta_p + \beta_d) b_w d \quad (15)$$

where: $\beta_p = (100A_s / b_w d)^{1/2} - 1$
 $\beta_d = (1000 / d)^{1/4} - 1$
 A_s : cross-sectional area of the tension reinforcement
 b_w : width of the beam
 d : effective depth of the beam (mm)
 f_c' : compressive strength of the concrete (MPa)

However, in the case of sandwich beams, the value of V_{co} was found to be around 0.6 of the value calculated by Eq.(15). This can be illustrated by the relationships between applied shear force and strain in the tie plates, as shown in Fig.34. In this figure, the strain measurements in the first loading cycle are plotted for two of the fatigue tests. The tie plate strains calculated by Eq.(13) are also shown by the dotted straight lines, using $N=1$ and the value of V_{co} calculated by Eq.(15). The solid lines are for a value of V_{co} equal to 0.6 of the value calculated by Eq.(15). There is a good agreement between the solid lines and the strain measurements in the first loading cycle. Hence, for the sandwich beams investigated in this study, the value of V_{co} is about 0.6 of the corresponding value for RC beams and defined as follows:

$$V_{co} = 0.6 \times 0.2 f_c'^{1/3} (1 + \beta_p + \beta_d) b_w d \quad (16)$$

where: $\beta_p = (100A_s / b_w d)^{1/2} - 1$
 $\beta_d = (1000 / d)^{1/4} - 1$
 A_s : cross-sectional area of the lower flange plate
 b_w : width of the sandwich beam
 d : effective depth of the sandwich beam (mm)
 f_c' : compressive strength of the concrete (MPa)

Thereafter, knowing the value of V_{co} , Eq.(13) was used to calculate the maximum strains at the centroid of the tie plates during fatigue tests. Also, Eq.(14) was used to calculate the strain ranges at the centroid

of the tie plates during the fatigue tests. **Figure 35** is a comparison between the maximum strains calculated by Eq.(13) and the maximum strains measured in two of the fatigue tests. Also, **Fig.36** is a comparison between the strain ranges calculated by Eq.(14) and the strain ranges measured in two of the fatigue tests. There is very good agreement between the strain measurements in the fatigue tests and the strains calculated by Eqs.(13) and (14), although the calculated values rise more than the measured values. Hence, it is concluded that Eqs.(13) and (14) can be used to predict the maximum strains and the strain ranges in the tie plates of the sandwich beams under fatigue loading. Note that these predicted strains are the strains at the centroid of the tie plate (i.e., excluding the effect of shear deformations of the tie plates).

Another significant point is to estimate the maximum strain and the strain range at point P, which is the most highly tensioned point in the tie plate (see **Fig.24**). In the fatigue tests on sandwich beams, point P was the origin of the fatigue crack in the tie plate. The strain at point P depends on the width of the tie plate. If the width of the tie plate is increased, the shear deformations of the tie plate increase, which in turn results in higher strain at point P. In the present study, the maximum strains and the strain ranges at point P were approximately three times greater than the corresponding values at the centroid of the tie plate.

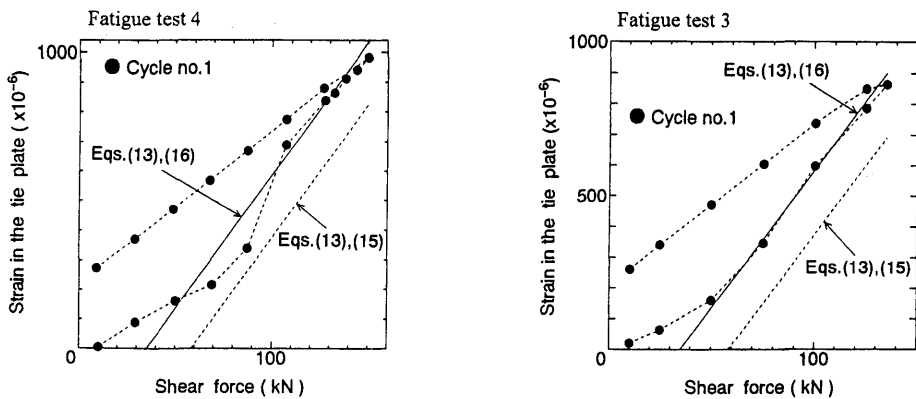


Fig.34 Relationship between Applied Shear Force and Strain in Tie Plates

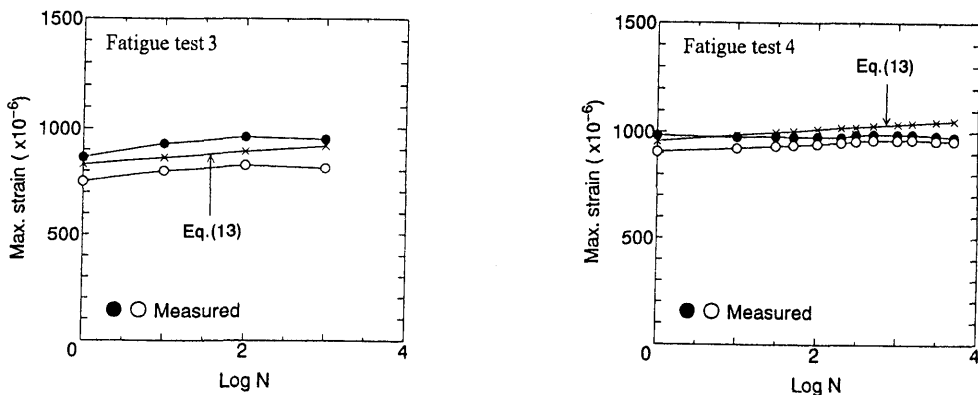


Fig.35 Comparison between Maximum Strains Calculated by Eq.(13) and Maximum Strains Measured in Fatigue Tests

6. DESIGN PROPOSAL FOR SANDWICH BEAMS

6.1 Sandwich Beam Without Shear Reinforcement

This section describes a procedure that can be used to design steel-concrete sandwich beams without

shear reinforcement under fatigue loading. The design procedure is outlined in the chart shown in Fig.37.

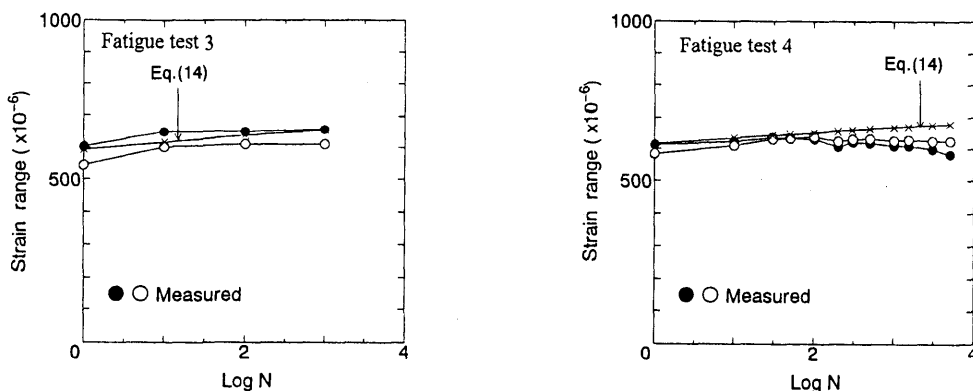


Fig.36 Comparison between Strain Ranges Calculated by Eq.(14) and Strain Ranges Measured in Fatigue Tests

The procedure can be summarized as follows:

- 1- Choose values of maximum and minimum fatigue load (P_{max} and P_{min}) considering actual loading conditions and decide on the required fatigue life of the sandwich beam (N_{req}).
- 2- Select the geometry of the sandwich beam and the material properties (i.e., the concrete compressive strength, the yield point, and the tensile strength of the steel plates).
- 3- Evaluate the static load-carrying capacity of the beam (P_u) either by the finite element method, by using a design code equation¹⁾, or by carrying out a static loading test.
- 4- Knowing the percentage of (P_{max} / P_u), the $S-N$ relationship in Fig.17a can be used to predict the fatigue life of the sandwich beam with failure due to concrete crushing.
- 5- Using bending theory, calculate the stress range in the tension steel plate at the maximum bending moment section, which conservatively approximates the average stress range at the potential fracture section of the tension steel plate.
- 6- Multiply this calculated stress range should by an amplification factor (α) to account for the effect of local bending deformations of the tension steel plate as well as the effect of shear transfer between the concrete and the tension steel plate. In the present study, this amplification factor (α) is approximately equal to 5.0.
- 7- Next, using the S_f-N relationship of the steel plate in air¹²⁾ (see Fig.18) and the stress range calculated in step 6, the fatigue life of the sandwich beam with failure due to fracture of the tension steel plate can be calculated as shown in Fig.18.
- 8- The shorter of the fatigue lives calculated in steps 4 and 7 should be selected as the fatigue life of the sandwich beam (N_f).
- 9- If N_f is less than the required fatigue life (N_{req}), the dimensions and material properties of the beam should be changed until N_f becomes equal to or greater than N_{req} .

6.2 Sandwich Beam With Shear Reinforcement

This section describes a procedure that can be used to design steel-concrete sandwich beams with shear reinforcement under fatigue loading. The design procedure is outlined in the chart shown in Fig.38. The design procedure can be summarized as follows:

- 1- Decide on values of maximum and minimum fatigue load (P_{max} and P_{min}) considering actual loading conditions and decide on the required fatigue life of the sandwich beam (N_{req}).
- 2- Select the geometry of the sandwich beam and the material properties (i.e., the concrete compressive strength, and the yield point and tensile strength of the steel plates).
- 3- Evaluate the static load-carrying capacity of the beam (P_u) either by the finite element method, by carrying out a static loading test, or by using a design code equation¹⁾.
- 4- Knowing the percentage of (P_{max} / P_u), the $S-N$ relationship obtained using the finite element method presented in this study as shown in Fig.30a can be used to predict the fatigue life of the sandwich beam

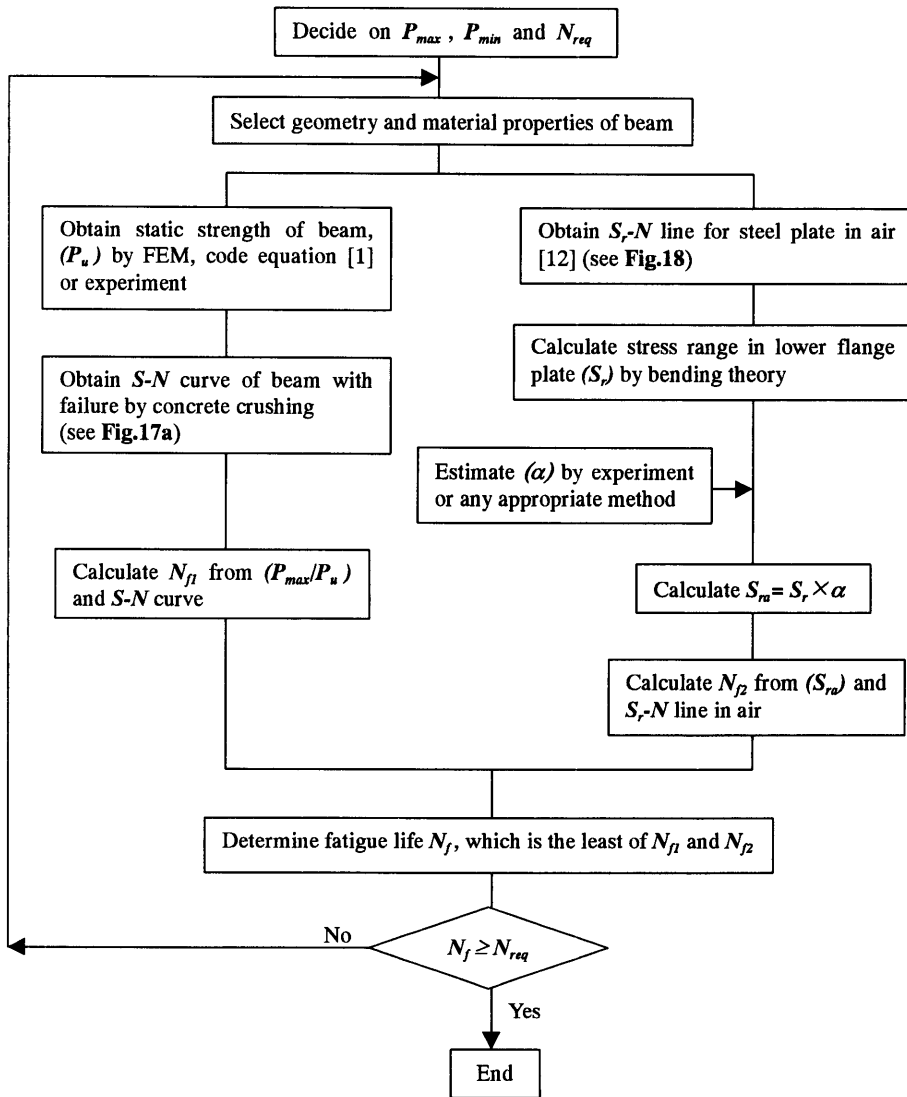


Fig.37 Design Procedure for Sandwich Beams without Shear Reinforcement

with failure due to concrete crushing.

5- Using conventional bending theory, the stress range in the lower flange plate at point W is calculated (see Figs.21a and 21b).

6- Multiply this calculated stress range at point W by an amplification factor (α) to account for the influence of local bending deformations of the flange plate (see Fig.21b) as well as the influence of shear transfer between the concrete and the lower flange plate. In the present study, this amplification factor (α) is approximately equal to 5.0.

7- Next, using the S_r - N relationship of the flange plate in air¹²⁾ (see Fig.32) and the stress range calculated in step 6, the fatigue life of the sandwich beam with failure due to fracture of the lower flange plate can be calculated as shown in Fig.32.

8- Using Eqs.(13), (14), and (16), the stress range at the centroid of the tie plate can be calculated.

9- Multiply this calculated stress range at the centroid of the tie plate by an amplification factor (γ) to account for the effect of shear deformations of the tie plate. In the present study, this amplification factor

(γ) is approximately equal to 3.0.

10- Now, using the S_r - N relationship of the tie plate in air¹³⁾ and the stress range calculated in step 9, the fatigue life of the sandwich beam failing due to fracture of the tie plate is calculated as shown in Fig.39.

11- The shortest of the fatigue lives calculated in steps 4, 7, and 10 should be selected as the fatigue life of the sandwich beam (N_f).

12- If N_f is less than the required fatigue life (N_{req}), the dimensions and material properties of the beam should be adjusted until N_f becomes equal to or longer than N_{req} .

The design procedure described here is applicable not only to case in this study but also to other cases of sandwich beams with tie plates. At this moment, it is necessary to conduct either an FEM analysis or a fatigue test due to the lack of data on S - N curves and amplification factors. FEM analysis, however, can save time and cost in obtaining the S - N curve as compared with a fatigue test.

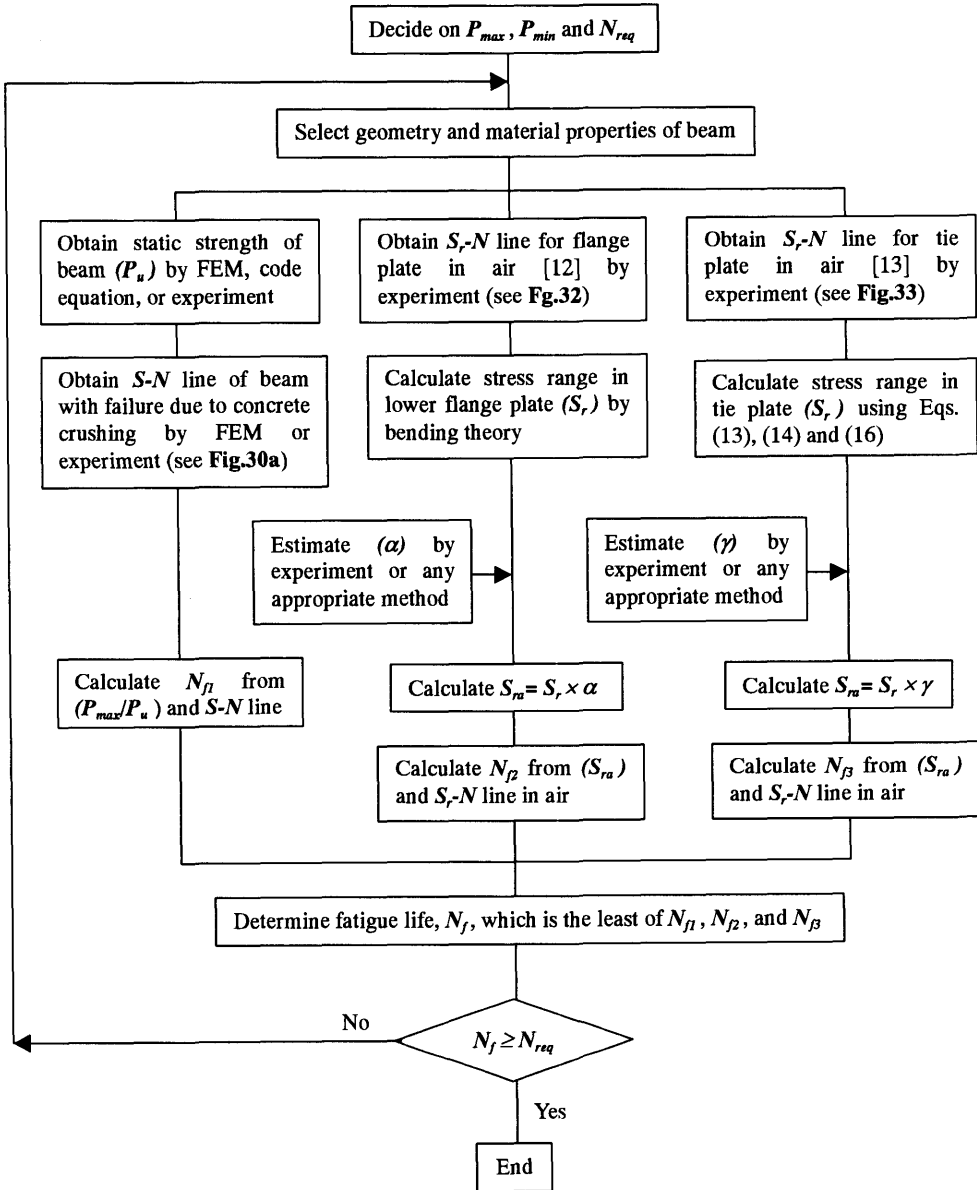


Fig. 38 Design Procedure for Sandwich Beams with Shear Reinforcement

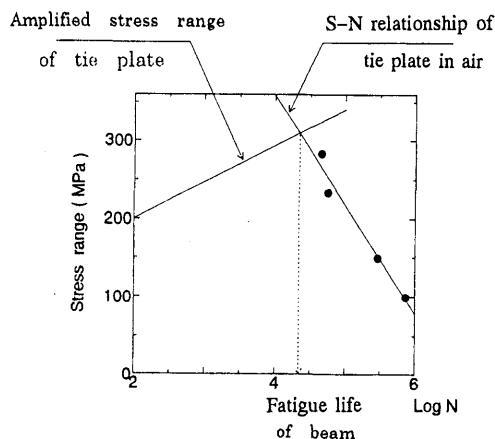


Fig.39 Prediction of Fatigue Life of Sandwich Beam which Fails due to Fracture of Tie Plate

7. CONCLUSIONS

7.1 Sandwich Beams without Shear Reinforcement

(1) For large maximum fatigue loads ($P_{max} = 65.5\%$, 70.7% , and 82.1% of the static strength), the failure mode of the beam is concrete crushing between diagonal cracks, whereas for smaller loads ($P_{max} = 49.0\%$ and 63.2% of the static strength), failure is fracture of the tension steel plate at the support point.

(2) The sandwich beam investigated in this study also exhibits a diagonal tension failure mode. In this case, the beam fails due to propagation of a main diagonal crack without any crushing of the core concrete. It was observed that the crack pattern affects the failure mode of the beam. The diagonal cracks always originate at shear connector locations and then these cracks propagate with increasing loading cycles. Therefore, it can be said that the arrangement of shear connectors affects the failure mode of the beam. However, further study is needed to clarify the shear fatigue behavior of sandwich beams in tension shear failure mode.

(3) The fatigue strength of beams with failure due to concrete crushing can be predicted using a finite element method in which the compressive strength, tensile strength, and stiffness of the concrete are reduced with increasing loading cycles (N) or increasing stress range (S_r). However, it is simply assumed that Eq.(1) is applicable to the biaxial state of stresses. Further study is necessary to prove this assumption by carrying out fatigue tests on concrete elements under biaxial stress conditions.

(4) The fatigue strength of beams with failure by steel plate fracture can be predicted using the finite element method. The stress range in the tension steel plate is multiplied by an amplification factor to account for the effect of local bending deformations of the steel plate as well as the effect of shear transfer between the concrete and tension steel plate. Then, for an input number of loading cycles, the S_r - N relationship of the steel plate in air [12] is used to check whether the steel plate fractures or not.

(5) Based on the results of this study, a design proposal is made for sandwich beams without shear reinforcement under fatigue loading is presented.

7.2 Sandwich Beams with Shear Reinforcement

(1) The sandwich beam with shear reinforcement investigated in this study exhibits a shear compression failure mode under static monotonic loading. This failure mode is characterized by diagonal cracking and concrete crushing.

(2) For a maximum fatigue load (P_{max}) ranging between 41.8% and 90.4% of the static strength of the sandwich beam, the failure mode of the beam is fracturing either the lower flange plate or the shear reinforcing steel plates. However, for a very large maximum load ($P_{max}=96.1\%$ of the static strength), the failure mode of the beam is concrete crushing.

(3) The fatigue strength of beams with failure by concrete crushing can be predicted using a finite element method in which the compressive strength, tensile strength, and stiffness of the concrete are reduced with increasing loading cycles (N) or increasing stress range.

(4) The fatigue strength of the beam with failure by flange plate fracture can be predicted using the finite element method described in this study. The stress range in the lower flange plate calculated by the finite element method is multiplied by an amplification factor to account for the effect of local bending deformations of the flange plate as well as the effect of shear transfer between the concrete and the lower flange plate. Then, for an input number of loading cycles, the S_r - N relationship of the flange plate in air^[12] is used to check whether the flange plate fractures or not.

(5) Under fatigue loading, the maximum stresses of the tie plates can be predicted by the finite element method described in this study. The minimum stresses or stress ranges, however, cannot be predicted accurately by the finite element method. Further study is necessary.

(6) The fatigue strength of beams with failure by tie plate fracture can be predicted using the simple method presented in **Section 5**. The stress range in the tie plate calculated using Eqs.(13), (14), and (16) is multiplied by an amplification factor to account for the effect of shear deformations of the tie plate. Then, for an input number of loading cycles, the S_r - N relationship of the tie plate in air [13] is used to check whether the tie plate fractures or not.

(7) A design proposal is made for evaluating the fatigue strength of sandwich beams with shear reinforcement based on the results of this study.

Notations

A_s	: cross-sectional area of tension reinforcement or lower flange plate
A_w	: cross-sectional area of tie plate
b_w	: width of beam
d	: effective depth of beam
E_c	: modulus of elasticity of concrete
E_f	: reduced modulus of elasticity of the concrete under fatigue loading
E_s	: modulus of elasticity of concrete under static loading
E_w	: modulus of elasticity of tie plate
f_c'	: compressive strength of concrete
f_{max}	: maximum stress
f_{min}	: minimum stress
f_t	: tensile strength of concrete
f_u	: static strength
G_c	: concrete shear modulus
N	: number of loading cycles
N_C	: number of loading cycles required to induce compression fatigue failure at concrete Gauss point
N_f	: fatigue life
N_F	: fatigue life
N_I	: input number of loading cycles
N_{req}	: required fatigue life of sandwich beam
N_T	: number of loading cycles required to induce tension fatigue failure at concrete Gauss point
P_{max}	: maximum fatigue load
P_{min}	: minimum fatigue load
P_u	: static load-carrying capacity of beam

$P_{u,exp}$: experimental ultimate failure load
$P_{u,FEM}$: analytical ultimate failure load
r	: ratio of applied minimum shear force to applied maximum shear force
R	: ratio of minimum stress to maximum stress
R_{max}	: ratio of principal tensile stress at maximum fatigue load to tensile strength
R_{min}	: ratio of principal tensile stress at minimum fatigue load to tensile strength
R_N	: percentage of fatigue life
S	: fatigue load or fatigue strength
S_{max}	: equivalent stress calculated using $\sigma_{m,max}$ and $\tau_{d,max}$
S_{min}	: equivalent stress calculated using $\sigma_{m,min}$ and $\tau_{d,min}$
S_r	: stress range
V_{max}	: applied maximum shear force
V_{min}	: applied minimum shear force
α	: amplification factor to account for effect of local bending deformations of tension steel plate
β	: reduction factor for concrete tensile stress in fatigue analysis
γ	: amplification factor to account for effect of shear deformations of tie plate
ϵ_t	: concrete tensile strain
ϵ_{tu}	: concrete tensile strain when softening starts
ϵ_{wmax}	: strain at centroid of tie plate at applied maximum shear force
ϵ_{wr}	: strain range at centroid of tie plate
σ_{cmax}	: principal compressive stresses of concrete Gauss point at maximum fatigue load
σ_{cmin}	: principal compressive stresses of concrete Gauss point at minimum fatigue load
$\sigma_{m,max}$: mean stress calculated using σ_{cmax} and σ_{tmax}
$\sigma_{m,min}$: mean stress calculated using σ_{cmin} and σ_{tmin}
σ_t	: concrete tensile stress
σ_{tmax}	: principal tensile stresses of concrete Gauss point at maximum fatigue load
σ_{tmin}	: principal tensile stresses of concrete Gauss point at minimum fatigue load
$\tau_{d,max}$: deviatoric stress calculated using σ_{cmax} and σ_{tmax}
$\tau_{d,min}$: deviatoric stress calculated using σ_{cmin} and σ_{tmin}

Acknowledgments

This study was conducted as a part of a doctoral dissertation by the second author submitted to Hokkaido University. The second author is indebted to the Japanese Ministry of Education, Science, Sports and Culture for the Monbusho Scholarship that provided valuable support. The authors are also grateful to Grant-in-Aid for Scientific Research (B) (No.06555123) which partially supported this study. Thanks are due to the members of the Department of Civil Engineering in Sumitomo Construction Co., Ltd., for providing the facilities to carry out the analytical studies in this research work.

References

- [1] JSCE Research Subcommittee on Steel-Concrete Sandwich Structures, "Design Code for Steel-Concrete Sandwich Structures – Draft", Concrete Library of JSCE, No.20, pp.1-21, December 1992
- [2] Yokota, H. and Kiyomiya, O., "Fatigue Behaviours of Steel-Concrete Hybrid Beams", Transactions of the JCI, Vol.11, pp.455-462, 1989
- [3] Kiyomiya, O. and Yokota, H., "Fundamental Mechanical Properties of Steel - Concrete Hybrid Beams for Marine Environment", Proceedings of the Third International Conference on Steel-Concrete Composite Structures, Fukuoka, Japan, pp.527-532, September 1991
- [4] Zahran, M., Kanaya, K., Ueda, T., and Kakuta, Y., "Shear-Fatigue Behavior of Steel-Concrete Sandwich Beams Without Web Reinforcement", Transactions of the JCI, Vol.16, pp.431-438, 1994
- [5] Zahran, M., Ueda, T., and Kakuta, Y., "Analytical Evaluation for the Fatigue Strength of Steel-Concrete Sandwich Beams Without Shear Reinforcement", Proceedings of the International Conference on Concrete Under Severe Condition, Sapporo, Japan, pp.1684-1693, August 1995
- [6] Okamura, H. and Maekawa, K., "Nonlinear Analysis and Constitutive Models of Reinforced Concrete", Gihodo Shuppan, Tokyo, pp.1-25, 1991
- [7] Pantaratorn, N., "Finite Element Analysis on Shear Resisting Mechanism of RC Beams",

Dissertation Submitted to the University of Tokyo, pp.74-102, March 1991

[8] Tepfers, R. and Kutti, T., "Fatigue Strength of Plain, Ordinary, and Lightweight Concrete", ACI Journal, Vol.76, No.5, pp.635-652, 1979

[9] Tepfers, R., "Tensile Fatigue Strength of Plain Concrete", ACI Journal, Vol.76, No.8, pp.919-933, 1979

[10] Holmen, J.O., "Fatigue of Concrete Structures", ACI, SP-75, Detroit, pp.71-110, 1982

[11] Bennett, E.W. and Raju, N.K., "Cumulative Fatigue Damage of Plain Concrete in Compression", The Proceedings of the Southampton 1969 Civil Engineering Materials Conference, 1089-1102, 1969

[12] Zahran, M., Ueda, T., and Kakuta, Y., "A Study on the Fatigue Fracture of Steel Plates in Steel-Concrete Sandwich Beams", Proceedings of the JSCE Conference, Vol.50, pp.232-233, 1995

[13] Zahran, M., Ueda, T., and Kakuta, Y., "A Study on the Fatigue Strength of Steel-Concrete Sandwich Beams with Shear Reinforcement", Proceedings of the JCI Conference, Vol.18, pp.1397-1402, 1996

[14] Ueda, T. and Okamura, H., "Behavior in Shear of Reinforced Concrete Beams Under Fatigue Loading", Journal of the Faculty of Engineering, University of Tokyo (B), Vol.XXXVII, No.1, 1983,pp.17-48